OUKA
Osaka University Knowledge Archive

Title	On Efficient Control for Power Systems with Randomly Distributed Solar Photovoltaic Generators
Author(s)	李, 鈺
Citation	大阪大学, 2017, 博士論文
Version Type	VoR
URL	https://doi.org/10.18910/67143
rights	
Note	

Osaka University Knowledge Archive : OUKA

https://ir.library.osaka-u.ac.jp/

Osaka University

Doctoral Dissertation

On Efficient Control for Power Systems with Randomly Distributed Solar Photovoltaic Generators

Yu Li

June 2017

Graduate School of Engineering
Osaka University

Abstract

The tremendous resource of solar energy makes solar photovoltaic (PV) generator as one of the most promising renewable energy sources for system integration. The fast-growing share of PV in the gross electricity generation delivers significant ecological and economic benefits to the world's sustainable development. However, large and rapid deployment of PV demands effective technology supports to maintain system power quality. One of the major power quality concerns is voltage stability due to power flows from grid-connected PV. To sustain voltage stability in power system under large and random PV integrations, this study focused on voltage regulation with reactive power injection from PV inverter. Statistical analyses of voltage stability were initially conducted on power system under various allocation patterns of PV generators. In addition, several decentralized control schemes of reactive power were applied on inverter to investigate their control performances. Analysis results showed random allocation of solar PV may harm voltage stability around the tail part of radial circuit lines, as well as connecting buses of circuit lines. In addition, control performances of decentralized control schemes were insufficient without considering whole balance of system power flow. Based on these analyses, an efficient control method of inverter reactive power was proposed from a centralized approach, which cared for both allocations of PV and reactive power injection of inverters. The centralized control model was derived from PV-enabled power flow equation, which was a linear model describing the influence of inverter reactive power injection on voltage magnitude change. Control objective was formulated as an optimization problem, which aimed to find the best fit of reactive power injection that minimizes system voltage variation. Sparse optimization method, named constrained least absolute shrinkage and selection operator (LASSO), was adapted on the formulated optimization problem. LASSO added ℓ^1-norm penalty on reactive power injection, which was expected to shrink the number of operating inverters for voltage control. Control performances and efforts of LASSO were investigated in power system under random integration of PV generators. The estimated solutions of reactive power injection showed that LASSO succeeded in selecting the least essential PV inverters for voltage regulation with respect to large and random integration of PV generators, while maintained control performances on voltage stability.

Acknowledgements

This work has been carried out since April 2013, at the Department of Mechanical Engineering, Osaka University. Working as a PhD student in Japan was a meaningful and challenging experience for me. Over the years, I become deep in debt of gratitude to many individuals for their support, encouragement and inspiration. It was hardly possible for me to thrive on my doctoral work without all these people, I wish to express my earnest gratitude to them here.

First and foremost, I wish to express my sincere gratitude to my supervisor Prof. Dr. Masato Ishikawa. It was only due to his valuable guidance, constructive critique and constant encouragement that I was able to complete my research work. His dedication to academic research and thirst for knowledge have made him an inspiration to me and so many others. I am grateful and respectful for his open-mindedness and kindheartedness to students, which make laboratory life much easier for me as a foreigner. Also, I wish to extend my heartfelt thanks to Prof. Dr. Koichi Osuka. I deeply appreciate the opportunity he has provided me to study in Japan. I wish to thank him for initially introducing me to the academic world, as well as encouraging me throughout this journey with his cheerful enthusiasm and extraordinary insight for academic research. I wish to especially thank Prof. Dr. Shigemasa Takai for providing his precious time as my committee member. I am grateful for his valuable comments and helpful suggestions on this work. Furthermore, my deepest gratitude must be recorded to Prof. Dr. Yasuhiro Sugimoto. I highly appreciate his support and guidance during my master's study. I also wish to thank him for carefully reading this manuscript and giving me insightful comments on this work.

Staff members and students in Ishikawa Lab and Osuka & Sugimoto Lab are so much like family to me. It was my privilege to spend time with so many sincere, motivated, and genuinely good people here. I have learnt so much from them both professionally and personally, and shared many wonderful experiences over these years. Thanks to them, I kept my smile even during the most challenging time. In particular, I would like to thank Prof. Dr. Yuki Minami for the discussion and support he gave me on this work. Also, I am thankful to Prof. Dr. Yuichiro Sueoka and Dr. Daisuke Nakanishi for their advice and encouragement on writing this manuscript. Moreover, I wish to express my sincere thanks to secretary of Ishikawa Lab Mrs. Ai Nakamura who has always been kind and supportive to me. Special thanks to my peers, Mr. Tetsuro Hirano and Mr. Yoichi Masuda, for their great company along this journey, which truly makes me feel stronger.

Finally, I wish to thank my parents and entire family for their unconditional love, support and patience. Thanks for always grounding me and being my home.

Contents

List of Figures

Chapter 1

Introduction

1.1 Research background

Power system has a long history of using fossil fuels to produce electric power [1]. As electricity is an essential energy source of modern life, the massive usage of non-renewable energy for electricity production has brought growing concerns on its harmful environmental impacts, such as air pollutions and global warming issues. Technologies promote to use renewable energy sources, such as solar, wind, geothermal, biomass and hydropower, as alternative choices for electric power generation [2–4]. The integration of renewable energy sources would deliver significant ecological and economic benefits to the world's sustainable development, and even increase electrification of the world's most rural areas. Based on the REN21 report, electric power generated from renewables reached a 24.5% share of global electricity production, and 19.3% share of global electricity consumption is from renewables [5]. Many countries have even set an ambitious goal to use 100% renewable energy to supply their power demand [6,7].

Among all types of the renewable energy sources, the tremendous resource of solar energy attracts incremental interests from business and academic communities, as well as government policy makers, because of its significant potential for long-term growth in global power production [8]. The power generation from solar photovoltaic systems (PV) is estimated to reach 11% of global electric power production by 2050 and reduce 2.3 gigatonnes (Gt) of CO_2 emissions per year [8]. For current status, global production of solar PV only achieves 1.5% [5]. Thus, high integration and rapid deployment of solar PV is predicted in the existing power system during next few decades, which will definitely require effective technology supports, in terms of power quality and system stability [9–12].

One of the major challenges associated with PV integration is to sustain voltage stability [10–19]. Voltage stability refers to the ability of power system to maintain voltage profile within permitted operation range, after disturbances such as load variations [20,21]. Grid-connected PV injects solar power generation to its connected power consumer, and delivers excess power to the utility grid as a reverse power flow. Directions of existing power flows are modified in power system with PV, which may result in voltage exceeding or decreasing beyond permitted operation limit [13–15]. In some cases, PV penetration improves voltage quality of poor voltage area to its stable state. For other cases, PV integration might cause severe voltage deviation, which leads to system blackouts and dramatic economic loss. Since growing numbers of PV generators connect with consumers in distribution system of the power network, voltage stability of the distribution system becomes major concern in this study.

In conventional distribution system, two types of voltage regulation methods are often applied to power system [22,23]. One is on-load tap-changing transformer (OLTC). Take a single circuit line as an example, voltage drops along the circuit line to deliver power from generator/substation to power consumers. In order to avoid voltage dropping lower than minimum permitted point, power system raises voltage at the delivery point with OLTC. The other one is static shunt compensator. Power is sorted into real and reactive power, the real power denotes energy transfer of power distribution, the reactive power denotes stored energy, which returns to source in a cycle. Power system needs to keep power balance of the real and reactive power between generators and consumers. It is understood that inability of power system to supply or absorb reactive power would cause voltage collapse [24]. Static shunt compensator ensures sufficient supply or absorption of reactive power to compensate reactive power demand from consumer loads. As a result, power system maintains voltage stability with reactive power regulation.

With small amount of PV integration, conventional voltage regulators are sufficient for voltage control [16]. For specific assigned PV generators, setting parameters of OLTC and shunt compensators can be calculated to plan optimal operation of the power system [25]. For strategically placed grid-connected PV generators, optimization algorithms have been developed to search optimal size, number and allocation of PV generators, which are subject to voltage operation limit [26–29]. As PV generators increasingly integrate with power system, high penetration of PV promotes growth of power demand from residential consumers. Then, the optimal allocation of PV becomes unpractical for a power system, as PV allocations are usually customers' choices [30]. In other words, the high penetration of PV induces randomness in the siting locations and patterns of PV, and as a consequence, increases vulnerability of voltage instability. The associated characteristics of voltage deviation raise concerns in this study.

Moreover, due to characteristics of PV, high integration of PV generators makes conventional voltage regulators insufficient to sustain voltage stability [16,19]. Power generation of PV varies with respect to weather conditions, such as solar radiation and temperature [31,32]. Since solar movement and weather forecasting technology is relatively well understood, much of the variation in PV generation is predictable during long periods of time. However, moving clouds might temporarily cover sunlight on PV cells, which is less predictable for short periods of time [11]. In consequence, uncertainty of short-time PV generation influences transient stability of its integrated power system [18,33]. When the integration of PV increases, conventional voltage regulators become less effective to control the rapid change induced by PV [16]. Reactive power control of PV inverter was considered an efficient approach to regulate voltage deviation in such situation, thanks to the characteristics of PV inverter [34–38]. As an essential component in grid-connected PV, PV inverter converts DC power of PV cells into AC power that compatible for consumer load and utility grid. Meanwhile, it generates reactive power which is considered an efficient control input to rapidly regulate voltage deviation. Options of control schemes for inverter were discussed in several studies [39–42]. Optimization algorithms were developed to compute reactive power output of inverter, which sustains voltage stability [36,43]. However, these previous studies have only focused on power system with pre-allocated PV. The control performance of inverter reactive power still demands investigation for power system with randomly integrated PV.

As randomness of PV integration challenges the voltage stability of power system, this study aims to analyze the characteristics of voltage variation and the control performance of PV inverter with respect to various allocation patterns of PV. With the associated analysis results, this study also aims to propose a reactive power control scheme for PV inverter, which is expected to robustly suppress voltage deviation in power system with random PV integration.

1.2 Research objective and contribution

Since exponentially growing integration of PV shift its allocation scenario from strategic planning to random siting, the associated voltage stability becomes one of the major concerns for massive PV penetration. This study aims to investigate the characteristics of voltage deviation with respect to random allocation of PV, as well as develop effective voltage control method in this condition.

To begin with this study, statistical and worst-case analyses of voltage stability is conducted under completely random allocation of PV generators. Radial distribution system is chosen as objective power system, since the simplicity of its network

configuration contributes to investigate the characteristics of voltage deviation with respect to various allocation patterns. The allocation patterns of PV are sorted as follows: random distribution of one or a few number of PV generators; uniform distribution of a large number of PV generators. The associated changes in voltage stability are analyzed with respect to allocation patterns. Moreover, basic control schemes of reactive power by Seal *et al.* and Turitsyn *et al.* [39,40], are applied on PV inverters, which aims to evaluate the control performance of inverter reactive power with respect to random allocation of PV generators. Furthermore, k-medoids clustering method is employed to partition the resulted data of voltage stability related analysis results [44], which divides similar voltage deviation of various PV allocation patterns into several clusters, and as a consequence, reduce the analysis pressure of big data volume.

Voltage stability analyses demonstrated above indicates that severe voltage deviation may occur under random allocation of PV generators [45]. Additionally, basic control schemes of inverter reactive power are unable to sustain voltage stability with respect to random allocation of PV [46]. Furthermore, the author wonders if all grid-connected PV generators have to conduct inverter reactive power control, in order to ensure voltage stability. According to IEEE standard 1547–interconnection standard of distributed resources with power system [47], reactive power support from distributed resources were not allowed concerning operation safety. Even though latest smart grid interoperability reference–IEEE standard 2030 established permission on control support from distributed resources [48], efficient control of inverter reactive power will still benefit the power system under large and random integration of PV, in terms of operation safety and cost.

To maintain voltage stability efficiently with respect to random allocation of PV, the author proposes to care for the importance of allocation of both PV generators and reactive power of PV inverters. A constrained linear relation between voltage magnitude change and reactive power change of PV inverter is derived from linearizing power flow equations with power integration from PV [26,49]. With the constrained linear model, control objective is formulated as to optimize the reactive power injection that minimizes voltage variation. In order to select the least essential inverters to increase the control efficiency, sparse optimization technique is adapted on the optimization problem. This sparse optimization method is named as constrained least absolute shrinkage and selection operator (LASSO) [50,51], which adds a ℓ^1-norm penalty and prior constraint on its regression coefficients–the reactive power change in this study. The ℓ^1-norm penalty contributes to shrink some estimates of the reactive power change towards zero and select fewer PV inverters to interpret the strongest feature of the provided model [52,53]. The prior constraint represents physical limitation of PV inverter. Same optimization problem is also solved with standard constrained least-square method. The resulting sparsity and effectiveness

of the constrained LASSO method are compared with the corresponding results from standard constrained least-square method, which indicates that the constrained LASSO approach succeeds in selecting least essential inverters to inject reactive power, without sacrificing control performance [54].

1.3 Dissertation overview

Overview of the manuscript is demonstrated below:

Chapter 2 briefly introduces grid-connected photovoltaic system, which includes the explanation of its main components and their respective feature. As two most important components of the grid-connected PV system, PV cell and inverter are described in detail in this chapter.

Chapter 3 demonstrates two types of power networks that are utilized in this study. One is radial distribution system. The other one is meshed distribution system. Radial distribution system is employed to conduct the statistical and worst-case analysis of voltage stability. Meshed distribution system is used to adapt the proposed efficient controller of inverter reactive power. In addition, power flow equations with PV power are introduced for both power systems, which contributes to compute voltage magnitudes in power system. Based on the power flow equations, reactive power control of PV inverter is introduced, where the benefits of using inverter reactive power are also explained.

Chapter 4 describes the study results on statistical and worst-case analyses of voltage stability, in power system under random distribution of PV generators. Several basic control schemes on inverter reactive power are induced here, which are applied on PV inverters to investigate their control performance with respect to various allocation patterns of PV. IEEE 33-bus power system is taken as benchmark example to conduct the investigation. Analysis results of voltage stability are demonstrated with respect to one or fewer number of PV generators integration, and uniform distribution of PV generators. In addition, clustering method is utilized in the analyses. Related study results were published in conference proceeding [45] and journal paper [46] respectively.

Chapter 5 proposes an efficient reactive power control scheme for voltage regulation in power system with high and random PV integration. Constrained linear relation between reactive power change and voltage magnitude change is derived from power flow equations. Control problem is formulated as to optimize the reactive power injection of PV inverter. Sparse optimization technique, named constrained LASSO method, is adapted on this control problem. Same problem is also solved with

standard constrained least-square optimization method, which contributes to compare the performance of the proposed controller. IEEE 39-bus and 57-bus benchmark power systems are chosen to conduct the analysis. Related study results were published in journal paper [54].

Chapter 6 summarizes the research objective and contributions of this study, as well as concludes the analysis results including statistical analysis of voltage stability under random PV integration and control performances of proposed inverter reactive power control scheme. Future works of this study are also discussed in this chapter.

Chapter 2

Grid-connected photovoltaic system

This chapter briefly introduces grid-connected PV, which includes features and characteristics of its components. Grid-connected photovoltaic system supplies solar power generation to its connected electricity consumer, and delivers excess power to utility grid [4]. A grid-connected PV system usually consists of an arrangement of several components, which includes PV cells, PV inverter(s), power conditioning unit, grid connection equipment and optional additional battery [4,32,55,56]. Figure 2.1 shows a typical configuration of grid-connected PV, which illustrates the connections of each component and the power flow from PV cells to consumer and utility grid.

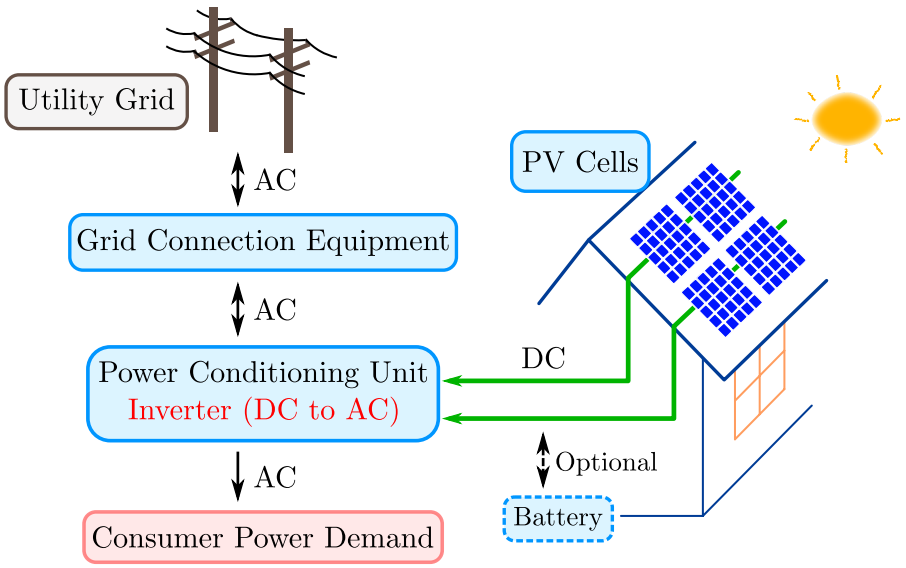

Figure 2.1: Typical configuration of grid-connected PV system

The associated features of each component are explained below:

- PV cells: Absorb sunlight to produce electrical power.
- PV inverter(s): Convert the generated electrical current from DC to AC.
- Power conditioning unit: Manage and improve power quality; PV inverter(s) are usually implemented in it.
- Grid connection equipment: Connect PV system with utility grid.

Solar radiation from sunlight triggers the PV cells to produce electric power, which is a DC power. The generated DC power injects into the power conditioning unit, where PV inverter(s) convert DC power to AC power, rest of the components in the unit collectively prepare compatible AC power to supply the consumer's power demand, and delivers excess power through the grid connection equipment into the utility grid.

PV cells and inverter(s) serve as the principal components for a grid-connected PV system, detail description of which are addressed in the following section.

2.1 PV cell model and characteristics

A PV cell converts energy of light into electrical power, which is the basic electrical unit to construct PV panels for commercial and residential applications. The power output of it primarily depends on solar radiation and cell temperature [31], and its performance could be explained with a well-known equivalent circuit of PV cell shown in Figure 2.2 [32,57,58]. This circuit could represent either an individual PV cell or a series of PV cells. PV cell is modeled as a current source in parallel with a diode and shunt resistance, the combined current of these components flows into a series resistance before delivering power generation into its connected consumer.

At given solar radiation and cell temperature, current (I)-voltage (V) relation in this circuit is expressed as:

$$\begin{aligned} I &= I_{\mathrm{L}} - I_{\mathrm{D}} - I_{\mathrm{sh}} \\ &= I_{\mathrm{L}} - I_0 \left[\exp\left(\frac{V + IR_{\mathrm{sh}}}{a}\right) - 1 \right] - \frac{V + IR_{\mathrm{s}}}{R_{\mathrm{sh}}} \end{aligned} \tag{2.1}$$

The parameters appear in Equation (2.1) represent: light current I_{L}, diode current I_{D} and its reverse saturation current I_0, shunt resistance R_{sh} and its corresponding current I_{sh}, series resistance R_{s}. Current I flowing through the series resistance and

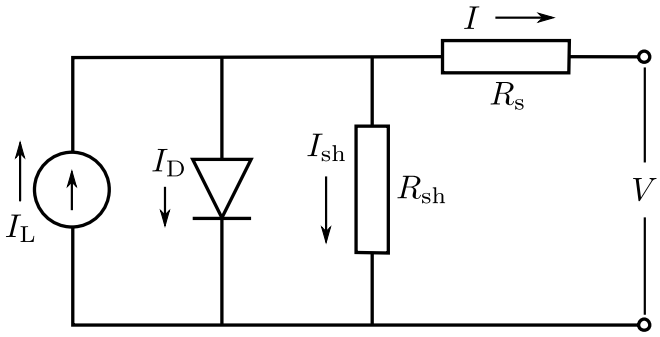

Figure 2.2: Equivalent circuit of PV cell

the respective voltage output V. In addition, a is called modified ideality factor, which is defined as:

$$a \coloneqq \frac{N_{\mathrm{s}} n_{\mathrm{I}} k T_{\mathrm{c}}}{q} \tag{2.2}$$

where N_{s} is the number of PV cells, n_{I} is ideality factor of diode to measure closeness the diode following the ideal diode equation, k is Boltzmann's constant (1.381×10^{-23}J/K) that defines the relation between average kinetic energy of each molecule and absolute temperature in a gas, T_{c} is cell absolute temperature, q is electron charge (1.602×10^{-19}coulombs).

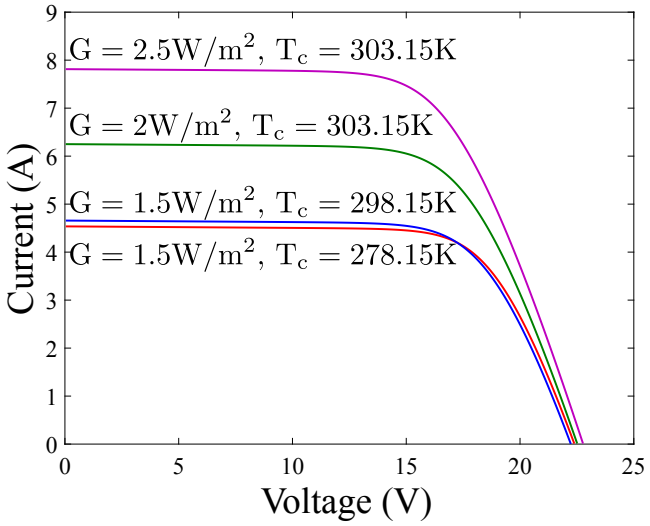

Figure 2.3: $I-V$ curves of PV

The parameters for computing the $I-V$ characteristics in Equation (2.1) are obtained from manufacturers and other known PV characteristics. Output of light current I_{L} depends on solar radiation G and cell temperature T_c. With the manufacture parameters from [57], G and T_c impacts on the $I-V$ characteristics of PV, Figure 2.3 shows $I-V$ characteristics in four different situations.

Power output of a PV cell is usually computed as:

$$P_{\mathrm{pv}} = IV \tag{2.3}$$

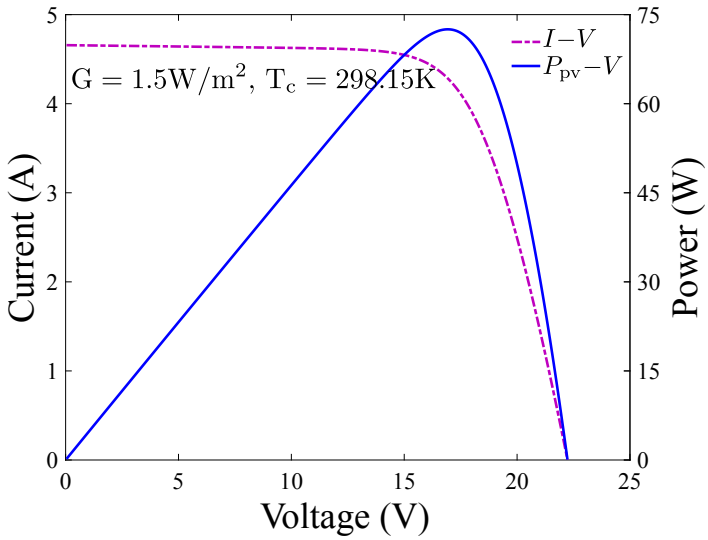

Figure 2.4: $I-V$ and $P_{\mathrm{pv}}-V$ curves of PV

With the manufacture parameters from [57], an example of the $I-V$ and $P_{\mathrm{pv}}-V$ curves is shown in Figure 2.4. Since nonlinear $I-V$ characteristics of PV varies with respect to atmospheric conditions, PV generator is usually equipped with maximum power point tracking (MPPT) controller to optimize its power conversion efficiency, and match the PV generation with the characteristics of the consumer load [4,59]. Although atmospheric conditions challenge the regulation techniques of the existing power system when integrating PV with it, for current stage of this research, power generation from PV is only considered as a constant and given value.

2.2 PV inverter

The DC power generated from PV flows into PV inverter to be converted to AC power, where it prepares the real power generation of PV compatible for grid connection and consumer charge. Meanwhile, PV inverter can generate reactive power in this process. The relation between real and reactive power in PV inverter is illustrated with Figure 2.5 [34,60].

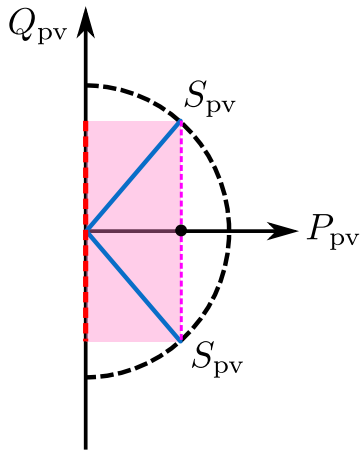

Figure 2.5: Mathematical model of PV inverter

In Figure 2.5, S_{pv} denotes apparent power of the PV inverter, which is determined by physical characteristics of inverter components. P_{pv} is real power generated by PV cells. Q_{pv} is reactive power generated by PV inverter. P_{pv} is marked with black bullet. The associated reactive power capability of inverter is marked with red dash line on vertical axis. Mathematical expression of the PV inverter is given as:

$$|Q_{\text{pv}}| \leq \sqrt{(S_{\text{pv}})^2 - (P_{\text{pv}})^2} = Q_{\text{max}} \tag{2.4}$$

where the reactive power capability of inverter is constrained by its apparent power capability S_{pv}. Let $|Q_{\text{max}}|$ be limitation of reactive power capability of PV inverter.

Chapter 3

Power flow and reactive power control of PV inverter

Power system is an interconnected network system which conducts generation, transmission, distribution and consumption of the electrical power. To ensure power quality of a system, power flow computes voltage magnitude and phase angle to determine the best operation of the network and plan future expansion of the power system. This study concentrates on distribution system of the power network to investigate voltage stability and inverter control method in power system with random PV integration. Two types of distribution networks are employed: one is radial distribution system, the other is meshed distribution system. When PV generation injects into power system, voltage magnitude and its phase angle at each bus is determined by solving the power flow equations. From the analyses of power flows, reactive power of PV inverter turns out to be a controllable input for voltage regulation, which is briefly described in the final section.

3.1 Power flow of radial distribution system

Radial distribution system is considered the simplest and cheapest power system. For a group of consumers, this system is featured with only one source of power generation and a tree-like network configuration, where consumer households radially distributed from power station and no looped network exists in it [61]. This type of power network is usually constructed in rural area with sparsely distributed consumers. Although a single error in one circuit line may interrupt the power quality of the whole system, the simplicity of the network contributes to analyze the characteristics

of voltage deviation and control performance of inverter reactive power, in power system with random PV integration.

The radial distribution system can be simplified as one line circuit shown in Figure 3.1. Assume there are n buses here, let $\mathcal{I}$ denote the set of bus indices. As mentioned above, only one energy source exists in the circuit, like a substation of the power system, set its bus index to 1. Complex power from bus 1, $P_1 + iQ_1$, flows into its adjacent bus along this circuit line, until it reaches the end of the circuit at bus n. Let bus index j be an arbitrary power consumer along the distribution line. Complex power delivered from bus j to bus $j+1$ is expressed as $P_j + iQ_j$, where P_j and Q_j are real and reactive power respectively. With the same principle, power distributed between two adjacent buses could be expressed as shown in Figure 3.1. Since bus n is the end of the circuit, there will be no power distributed from it, $P_n + iQ_n$ is zero. Additionally, when consumer charges power $P_{d,\,j+1} + iQ_{d,\,j+1}$ from bus $j+1$, bus $j+1$ extracts it from power of the upper stream $P_j + iQ_j$.

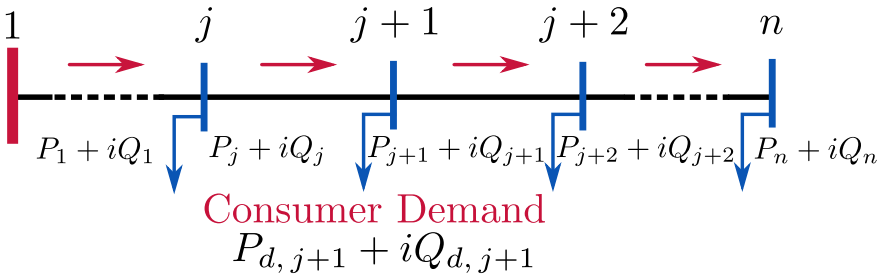

Figure 3.1: Single line radial distribution circuit

According to Ohm's law, power flow equations of the radial distribution system are formulated below [62,63]:

$$\begin{aligned} P_{j+1} &= P_j - r_j \frac{P_j^2 + Q_j^2}{|V_j|^2} - P_{d,\,j+1} \\ Q_{j+1} &= Q_j - x_j \frac{P_j^2 + Q_j^2}{|V_j|^2} - Q_{d,\,j+1} \\ V_{j+1}^2 &= V_j^2 - 2(r_j P_j + x_j Q_j) + (r_j^2 + x_j^2)\frac{P_j^2 + Q_j^2}{V_j^2} \end{aligned} \tag{3.1}$$

where $j \in \mathcal{I}$; V_j is voltage magnitude at bus j, $r_j + ix_j$ is complex impedance of circuit line between bus j and $j+1$. This power flow method is originally utilized to analyze

capacitor placement and sizing in radial distribution system, the computation above is simple when it comes to adjusting the injection of reactive power [62–64].

3.2 Power flow of meshed distribution system

Meshed distribution system is the most complex and expensive power system. Multiple sources of power generation supply consumer households in an interconnected network system, where one consumer bus could be supplied with multiple generators simultaneously [61]. This system is often built in downtown area with high load demand, since the complex network structure adds more reliability to the power system.

Meshed distribution power system could be considered as multiple radial circuit lines like Figure 3.1 interconnected with each other. The power flow equations of this system are formulated to balance power injection at each bus. Figure 3.2 shows an illustration of nodal power injection. For each nodal bus, the nodal power injections (P, Q) are equal to the net power of extraction from consumers (P_d, Q_d) and injection from generators (P_g, Q_g).

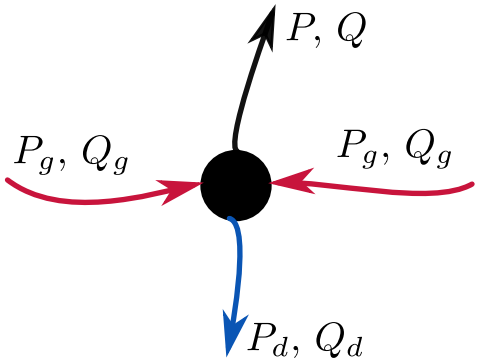

Figure 3.2: Illustration of nodal power injection

Assume a meshed power system consists of n buses and m generators. Let the set of bus indices be $\{1, \cdots, n\}$, buses are sorted into three types:

- Reference bus: One generator bus is chosen as reference bus for power flow study. Let $\mathcal{I}_{\text{ref}}$ denote the set of bus index.
- Generator buses: Power generators are installed at these buses, where real power generation and voltage magnitude are assumed constant and given. Let $\mathcal{I}_g$ denote the set of bus indices, which includes $(m-1)$ buses.

- Consumer buses: Electrical power are demanded at these buses, where real and reactive power are determined constant value at the operating point. Let $\mathcal{I}_d$ denote the set of bus indices (the subscript "d" stands for "demand".), which has $(n-m)$ buses.

The power flow equations are formulated as [65]:

$$\begin{bmatrix}\Delta P\\ \Delta Q\end{bmatrix} = \begin{bmatrix}P(\Theta,V)+P_d-P_g\\ Q(\Theta,V)+Q_d-Q_g\end{bmatrix} = 0 \tag{3.2}$$

$$P_f(\Theta,V) = V_f\sum_{t=1}^{n} V_t(G_{ft}\cos\theta_{ft}+B_{ft}\sin\theta_{ft}), \quad \forall f\in\mathcal{I}_d\cup\mathcal{I}_g \tag{3.2a}$$

$$Q_c(\Theta,V) = V_c\sum_{t=1}^{n} V_t(G_{ct}\sin\theta_{ct}-B_{ct}\cos\theta_{ct}), \quad \forall c\in\mathcal{I}_d \tag{3.2b}$$

In Equation (3.2), V is vector of voltage magnitudes; Θ is vector of voltage phase angles; P, Q are vectors of real and reactive power injections of nodal buses; P_g, Q_g are vectors of real and reactive power generation at generator buses; P_d, Q_d are vectors of real and reactive power demand at consumer buses. The equations of nodal power balance can be further expanded as Equation (3.2a) and Equation (3.2b); P_f, Q_c are the real power and reactive power balance at bus f, s; G_{ft}, G_{ct}, B_{ft}, and B_{ct} are real and imaginary parts of element in bus admittance matrix; θ_{ft}, θ_{st} are differences of voltage angles between the two index buses. Equation (3.2) solves all unknown voltage magnitudes and angles in the meshed power system. Note Equation (3.2) generally solve power flow problems in all types of power systems. Matpower software is employed to solve the power flow equations in this study [66].

3.3 Integration of PV power

When PV generators integrates with power system, power generation of PV injects into the PV-enabled consumer buses to compensate the power demand of consumer, then excess power of PV is delivered into the utility grid. These processes can be reflected on power flow equations by modifying the power demand of PV-enabled consumer buses.

For radial distribution system, PV-enabled power flow equations are described as:

$$P_{j+1} = P_j - r_j \frac{P_j^2 + Q_j^2}{|V_j|^2} - (P_{d,\,j+1} - P_{\mathrm{pv},\,j+1}) \tag{3.3a}$$

$$Q_{j+1} = Q_j - x_j \frac{P_j^2 + Q_j^2}{|V_j|^2} - (Q_{d,\,j+1} - Q_{\mathrm{pv},\,j+1}) \tag{3.3b}$$

$$V_{j+1}^2 = V_j^2 - 2(r_j P_j + x_j Q_j) + (r_j^2 + x_j^2) \frac{P_j^2 + Q_j^2}{V_j^2} \tag{3.3c}$$

where $P_{\mathrm{pv},\,j+1}$ and $Q_{\mathrm{pv},\,j+1}$ are real and reactive power generation of PV at bus $j+1$ respectively. If PV doesn't exist at bus $j+1$, set them to zero.

For meshed distribution system, PV-enabled power flow equations are given as:

$$\begin{bmatrix} \Delta P \\ \Delta Q \end{bmatrix} = \begin{bmatrix} P(\Theta, V) + (P_d - P_{\mathrm{pv}}) - P_g \\ Q(\Theta, V) + (Q_d - Q_{\mathrm{pv}}) - Q_g \end{bmatrix} = 0 \tag{3.4}$$

where P_{pv} and Q_{pv} are vectors of real and reactive power from PV generators respectively.

Equation (3.3) and Equation (3.4) compute voltage deviates with respect to the power integration of PV. As real power generation of PV is considered constant and given in this study, reactive power of PV becomes the only controllable variable for voltage regulation.

3.4 Reactive power control of PV inverter

Historically, static shunt compensators and OLTCs have been used to maintain voltage stability of power systems. However, these voltage regulators are not fast enough to suppress transient voltage deviation induced by PV [16,36]. As shown in Table 3.1, reactive power of PV appears to be the only adjustable variable in power flow equations, which potentially suits for voltage regulation of PV-enabled power system.

Several studies have proposed to utilize reactive power of PV for voltage regulation [34–43]. Reactive power control of PV inverter has been considered a fast and cost efficient approach to ensure voltage stability: First, PV inverter is capable to cope with the rapid change of PV generation; Second, PV inverter is implemented in PV generator; As PV generator is deployed near power consumers, which enables inverter to deliver reactive power in short distance. In consequence, reactive power control of PV inverter costs less transportation losses; Third, PV inverter is allocated along

with PV generator in a decentralized rule, which will save land space and installation cost, rather than assigning extra regulators for voltage control.

Table 3.1: Parameters and variables in power flow equations

Parameters	**Description**	**Feature**
	Radial distribution system	
P_j	Net real power injection from bus j	$P_n = 0$
Q_j	Net reactive power injection from bus j	$Q_n = 0$
$r_j + ix_j$	Impedance of circuit line j	Given
$P_{d,\,j+1}$	Real power demand at bus $j+1$	Given
$Q_{d,\,j+1}$	Reactive power demand at bus $j+1$	Given
$P_{\mathrm{pv},\,j+1}$	PV real power at bus $j+1$	Given
V_j	Voltage magnitude at bus j, $V_1 = 1$p.u.	Solve
$Q_{\mathrm{pv},\,j+1}$	PV reactive power at bus $j+1$	Adjustable
	Meshed distribution system	
P	Vector of nodal net real power injection	$P = P_g - (P_d - P_{\mathrm{pv}})$
Q	Vector of nodal net reactive power injection	$Q = Q_g - (Q_d - Q_{\mathrm{pv}})$
$Y = G + iB$	Elements of system admittances (buses and branches)	Given
P_g	Vector of generator real power	Given
V_g	Vector of generator voltage magnitudes	Given
P_d	Vector of consumer real power demand	Given
Q_d	Vector of consumer reactive power demand	Given
P_{pv}	Vector of PV real power	Given
Θ	Vector of voltage phase angles	Solve
V_d	Vector of consumer voltage magnitudes	Solve
Q_{pv}	Vector of PV reactive power	Adjustable

Let $\mathcal{H}$ denote indices set of PV-enabled buses, k be an arbitrary index of PV-enabled buses, $[V_a, V_b]$ be permitted operation range of voltage. Control strategy of inverter reactive power can be formulated as follows:

$$\begin{aligned} &\text{Objective: } V_j \in [V_a, V_b], \quad j \in \mathcal{I} \\ &\text{Input: } Q_{\text{pv},k} \in \{|Q_{\text{pv},k}| \leq \sqrt{(S_{\text{pv},k})^2 - (P_{\text{pv},k})^2} = Q_{\text{max},k}\}, \quad k \in \mathcal{H} \end{aligned} \tag{3.5}$$

Equation (3.5) indicates that the control strategy of inverter reactive power is to adjust control input $Q_{\text{pv},k}$, in order to regulate voltage magnitude of each bus V_j within $[V_a, V_b]$. Several studies have designed control input $Q_{\text{pv},k}$ as function of voltage state to maintain voltage stability [39–42]. Other studies have developed optimization algorithms to compute control input $Q_{\text{pv},k}$, in favor of voltage stability [36,43]. Previous studies mainly focused on the power system with pre-assigned PV generators. The author wonders how these control strategies of previous studies would perform with respect to random PV allocation? how to efficiently determine the control input $Q_{\text{pv},k}$ in power system like this? The following chapters of this manuscript aim to answer these questions, and propose efficient control scheme for PV inverter to ensure voltage stability in this condition.

Chapter 4

Statistical analysis of voltage stability

With the knowledge on power flow study and inverter reactive power control, statistical and worst-case analyses of voltage stability are conducted on radial distribution system. PV generators are randomly integrated with the power network: random distribution of fixed number of PV; uniform distribution of a large number of PV. Besides, several basic controllers of inverter reactive power are applied on PV. The analyses on voltage stability are conducted under situations with or without inverter controls, which aim to investigate the challenges as well as benefits of reactive power control, with respect to large and random PV integration.

4.1 Basic control schemes

To begin with the analyses, several basic control schemes on inverter reactive power are introduced here. According to Seal *et al.* [39] and Turitsyn *et al.* [40], autonomous control mode of inverter reactive power injection can be managed based on the capability of inverter, and locally observed system voltage. In other word, reactive power injection of PV inverter can be designed as a function of local system voltage or power demand of consumers, that constrained by the power capability of inverter. The basic control modes of inverter are expected to sustain voltage stability with respect to large and random PV integration.

4.1.1 Direct compensation

In the radial distribution system, a very direct way to suppress the voltage variation is to minimize the difference of voltage magnitude between adjacent buses along circuit

lines [40]. Equation (3.3c) hints that $V_{j+1} \approx V_j$ will be realized when its left term equals to zero. As $(P_j^2 + Q_j^2)/V_j^2$ is a considerably small value compared with P_j and Q_j, it can be approximated as zero. Then, to reduce voltage variation between adjacent buses, the following requirement should be met:

$$r_j P_j + x_j Q_j = 0, \quad j \in \mathcal{I} \tag{4.1}$$

Note that r_j and x_j are resistance and reactance of circuit lines respectively, the ratio of r_j/x_j is usually constant. Based on this constraint, substitute Equation (4.1) for Equation (3.3a) and Equation (3.3b), which leads to:

$$Q_{\mathrm{pv},\,j+1} = \frac{r_j}{x_j}(P_{d,\,j+1} - P_{\mathrm{pv},\,j+1}) + Q_{d,\,j+1}, \quad j \text{ and } j+1 \in \mathcal{I} \tag{4.2}$$

As mentioned in Section 2.2, $Q_{\mathrm{pv},\,j+1}$ is constrained by the capability of inverter as Equation (2.4). Thus, when the computed result of Equation (4.2) exceeds its limitation, set $Q_{\mathrm{pv},\,j+1} = \pm Q_{\max}$.

4.1.2 Function design of inverter control mode

Another basic approach is to directly design control functions of reactive power injection with respect to local voltage state [39]. Several control schemes proposed by Seal *et al.* and Turisyn *et al.* are introduced below [39,40]:

Piecewise affine feedback

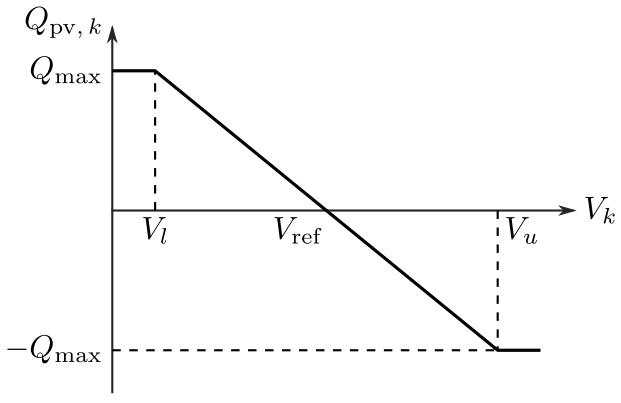

Figure 4.1: Piecewise affine feedback

In Seal's proposal [39], reactive power injection of inverter can be managed in several pre-designed control modes. One prototype configuration of the control mode is shown in Figure 4.1, where reactive power of $Q_{\mathrm{pv},k}$ and local voltage V_k are in a linear relation until $Q_{\mathrm{pv},k}$ reaches its power capability. The associated control function is described as:

$$Q_{\mathrm{pv},k} = \begin{cases} Q_{\max}, & \text{if } V_k \le V_l \\ Q_{\max}\dfrac{V_k - V_{\mathrm{ref}}}{V_l - V_{\mathrm{ref}}}, & \text{if } V_l < V_k < V_{\mathrm{ref}} \\ 0, & \text{if } V_k = V_{\mathrm{ref}}. \\ -Q_{\max}\dfrac{V_k - V_{\mathrm{ref}}}{V_u - V_{\mathrm{ref}}}, & \text{if } V_{\mathrm{ref}} < V_k < V_u \\ -Q_{\max}, & \text{if } V_k \ge V_u \end{cases}, \ k \in \mathcal{H} \tag{4.3}$$

Where V_l, L_l, L_u and V_u are constant parameters that determines the timing of switching control input $Q_{\mathrm{pv},k}$; k denotes the index of PV-enabled bus. This control scheme is named as piecewise affine feedback.

Smoothed switching

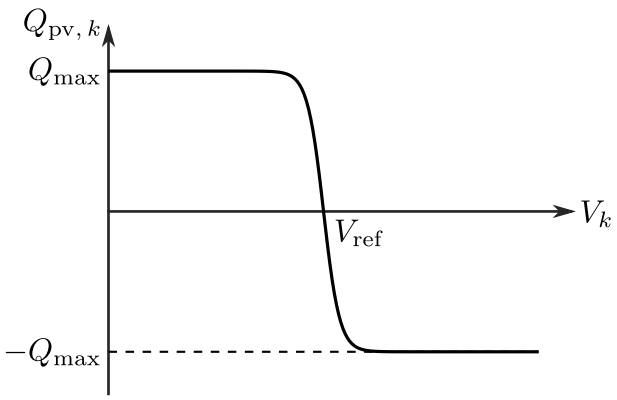

Figure 4.2: Smoothed switching

Turitsyn *et al.* simplifies the previous control function into a sigmoid function [40], which leads to:

$$Q_{\mathrm{pv},k} = Q_{\max}\left(1 - \frac{2}{1 + \exp(-4(V_k - V_{\mathrm{ref}})/\delta)}\right), \ k \in \mathcal{H} \tag{4.4}$$

This control scheme is named as smoothed switching here. V_{ref} denotes reference voltage. δ is a parameter that defines the shape of the curve. $V_{\text{ref}} = 1\text{p.u.}$ and $\delta = 0.04$ is chosen to resemble control schemes of piecewise affine feedback, which is shown in Figure 4.2.

Smoothed switching with binding boundary

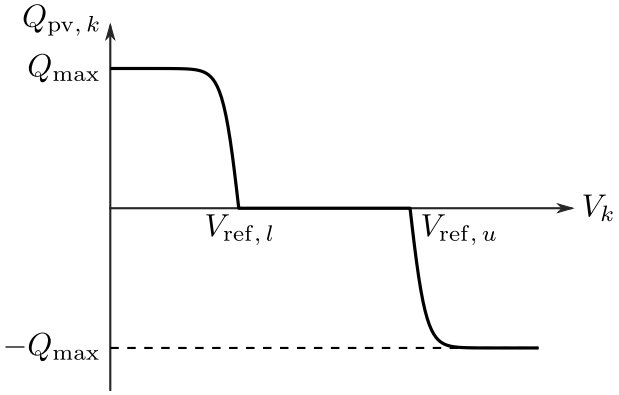

Figure 4.3: Smoothed switching with binding boundary

Smoothed switching (S-S) with binding boundary method is a modification of smoothed switching method by this study, where it changes the reference voltage V_{ref} in previous method to two separate value, $V_{\text{ref},\,l}$ and $V_{\text{ref},\,u}$ Figure 4.3. The resulted control function is described as:

$$Q_{\text{pv},\,k} = \begin{cases} Q_{\max}(1 - \dfrac{2}{1+\exp(-4(V_k - V_{\text{ref},\,l})/\delta)}), & \text{if } V_k \le V_{\text{ref},\,l} \\ 0, & \text{if } V_{\text{ref},\,l} < V_k < V_{\text{ref},\,u} \\ Q_{\max}(1 - \dfrac{2}{1+\exp(-4(V_k - V_{\text{ref},\,u})/\delta)}), & \text{if } V_k \ge V_{\text{ref},\,u} \end{cases}, \quad k \in \mathcal{H} \tag{4.5}$$

Control modes of inverter reactive power in Section 4.1 are designed as decentralized controllers for voltage regulation, which change control input Q_{pv} based on minimal local information at the connected consumer bus. The purpose of designing these methods is to maintain voltage stability autonomously by grid-connected PV when large number of PV generators randomly integrated with power system.

4.2 Description of benchmark power system

IEEE 33-bus distribution power system is chosen as benchmark example. which is a typical radial distribution power system used in studies of voltage regulation [64,67]. Due to the simple tree-like network configuration, it is easier to capture the characteristics of voltage deviation with respect to various allocation patterns of PV, as well as evaluate the effectiveness of reactive power control. In the 33-bus power system, generator bus 1 supplies 32 consumer buses, and 32 branches exists in it [67]. The network configuration of this system is shown in Figure 4.4, base voltage and power are 12.6kV and 100MVA respectively. Table 4.1 lists power demand and branch impedance data of 33-bus power system.

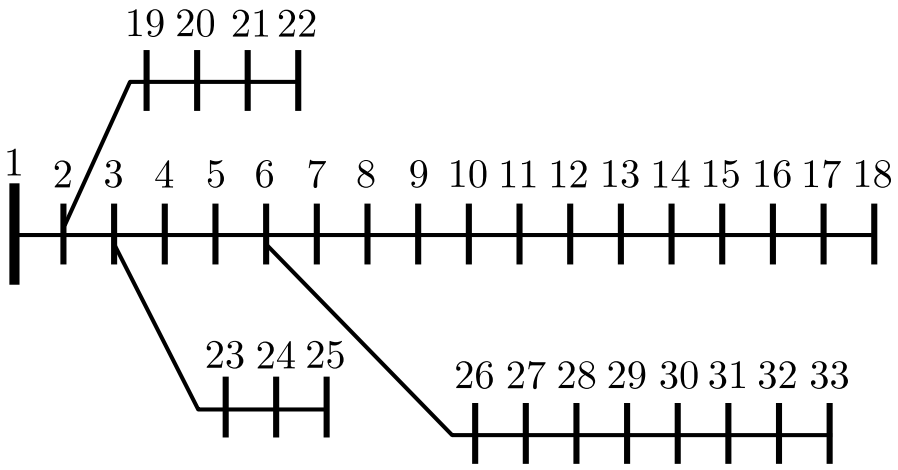

Figure 4.4: Network configuration of IEEE 33-bus power system

Table 4.1: Bus and branch data in 33-bus power system

Bus data			**Branch data**			
Bus	P_d (kW)	Q_d (kVAr)	From	To	r (Ω)	x (Ω)
1	0	0	1	2	0.0922	0.0470
2	100	60	2	3	0.4930	0.2511
3	90	40	3	4	0.3660	0.1864
4	120	80	4	5	0.3811	0.1941
5	60	30	5	6	0.8190	0.7070
6	60	20	6	7	0.1872	0.6188

(Continued on next page)

Table 4.1: (Continued)

Bus data			**Branch data**			
Bus	P_d (kW)	Q_d (kVAr)	From	To	r (Ω)	x (Ω)
7	200	100	7	8	0.7114	0.2351
8	200	100	8	9	1.0300	0.7400
9	60	20	9	10	1.0440	0.7400
10	60	20	10	11	0.1966	0.0650
11	45	30	11	12	0.3744	0.1238
12	60	35	12	13	1.4680	1.1550
13	60	35	13	14	0.5416	0.7129
14	120	80	14	15	0.5910	0.5260
15	60	10	15	16	0.7463	0.5450
16	60	20	16	17	1.2890	1.7210
17	60	20	17	18	0.7320	0.5740
18	90	40	2	19	0.1640	0.1565
19	90	40	19	20	1.5042	1.3554
20	90	40	20	21	0.4095	0.4784
21	90	40	21	22	0.7089	0.9373
22	90	40	3	23	0.4512	0.3083
23	90	50	23	24	0.8980	0.7091
24	420	200	24	25	0.8960	0.7011
25	420	200	6	26	0.2030	0.1034
26	60	25	26	27	0.2842	0.1447
27	60	25	27	28	1.0590	0.9337
28	60	20	28	29	0.8042	0.7006
29	120	70	29	30	0.5075	0.2585
30	200	600	30	31	0.9744	0.9630
31	150	70	31	32	0.3105	0.3619
32	210	100	32	33	0.3410	0.5302
33	60	40				

With Equation (3.1), Figure 4.5a shows the solved power flow of 33-bus power system. Bus 1 delivers real and reactive power to each consumer which are shown with red and black bar respectively. Blue and yellow bar shows the power demand at each consumer bus. In the absence of PV generator, voltage profile is shown in Figure 4.5b. The permitted range of voltage is from 0.9p.u. to 1.1p.u., voltage of each bus

stay in the permitted range without PV power. Voltage drops along each circuit line, as energy losses between adjacent buses.

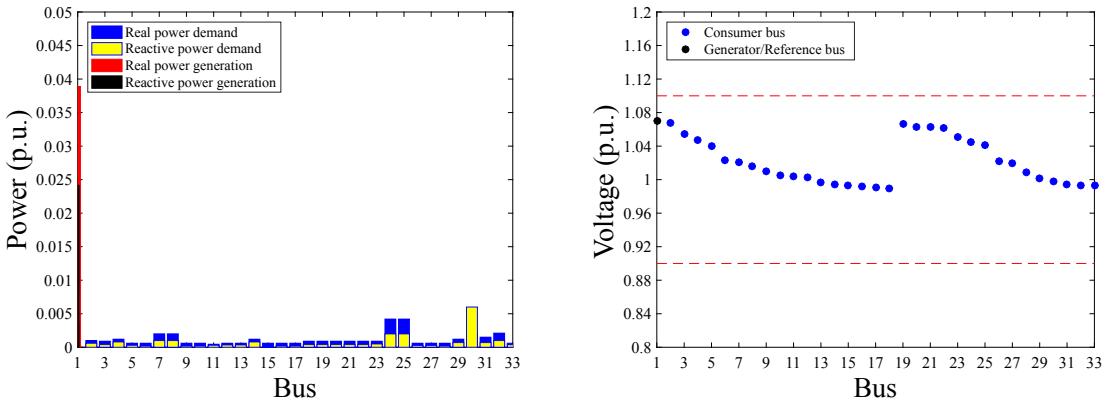

(a) Power flow data (b) Voltage profile without PV generation

Figure 4.5: IEEE 33-bus radial distribution system

4.3 Analyses on voltage stability

Voltage stability due to PV integration is analyzed on the 33-bus power system in two cases: one case is random distribution of fixed number of PV generators; The other case is uniform distribution of a large number of PV generators. Moreover, basic control schemes are applied on PV, in order to investigate the control performance of decentralized reactive power control under random PV integration. Assume apparent power generation of PV $S_{\text{pv}} = 1.1P_{\text{pv}}$, while the total active power generation of PV is 50% of total consumer active power demand. Active power generation of single PV is determined as: For the fixed number of PV generators case, number of PV is changed from 1 to 6; For the large number of PV generators case, active power and apparent power of PV are $P_{\text{pv}} = 2\text{kW}$ and $S_{\text{pv}} = 2.2\text{kVA}$ [60]. According to Equation (2.4), the allowable reactive power output is bounded in the range $|Q_{\text{pv}}| \leq 0.45P_{\text{pv}}$.

The parameter settings of each controller are listed in Table 4.2. Direct compensation method aims to minimize the difference of voltage magnitude from its upper stream bus. Piecewise Affine Feedback control and Smoothed Switching control method both set reference voltage to 1 p.u., and PV-enabled buses adjust the output of reactive power while bus voltage below/above this value. Smoothed Switching with Binding Boundary control method changes the reference voltage to upper and lower

permitted voltage in power system, and generates reactive power only when voltage at PV-enabled buses beyond the bounding of voltage.

Table 4.2: Parameter Settings in Controllers

Control Scenario	**Character/Parameter**
Direct Compensation	$Q_{\mathrm{pv},k} = \frac{r_k}{x_k}(P_{d,j} - P_{\mathrm{pv},j}) + Q_{d,k}$, k (To bus) $\in \mathcal{H}$, j (From bus) $\in \mathcal{D}$
Piecewise Affine Feedback	$V_{\mathrm{ref}} = 1$, $V_l = 0.97$, $V_u = 1.05$
Smoothed Switching (S-S)	$V_{\mathrm{ref}} = 1$, $\delta = 0.04$
S-S with Binding Boundary	$V_{\mathrm{ref},l} = 0.97$, $V_{\mathrm{ref},u} = 1.05$, $\delta = 0.04$

4.3.1 Random allocation of few PV generators

In this case, PV generator is allocated according to the following rules.: First, fix the net power generation from PV as 50% of net power demand; Second, divide the net power generation of PV by a pre-set number of PV generators; Third, apply inverter reactive power control schemes to evaluate voltage deviation with respect to various PV allocation patterns.

For all potential siting locations of PV, voltage variation forms an error-bar of deviation range at each bus. Figure 4.6a shows the voltage deviation when there is 1 PV generator integrated with power system. The black bullets in this figure represents the voltage profile in the absence of PV. Error-bars of voltage variation are shown in different color with respect to with/without control cases. The blue dashed lines represent the permitted voltage operating limitation.

The characteristics of voltage deviation in Figure 4.6 are as follows: First, consumer buses along longer circuit lines tend to have larger voltage deviation than those along shorter circuit lines. Second, severe voltage rise occurs without reactive power control. Decentralized reactive power control schemes only suppress voltage deviation in certain extend. Third, the error-bars of voltage deviation with control schemes result in the same range due to the limitation of inverter reactive power capability.

Frequency of voltage deviation with respect to various PV allocation patterns is plotted with color-bars in Figure 4.6. Darkness of color represents the frequency of voltage deviations, where frequency means the occurrence of situation. Figure 4.6b shows the color-bar in no control case, where severe voltage deviation occurs at the

tail parts of circuit lines than other controller cases. Voltage deviations are suppressed in the other cases with reactive power control. For all the with/without control cases, voltage deviation frequently occurs at connecting buses between lateral circuit lines and the upper stream of the feeder circuit line, (bus 19, 23, and bus 2, bus 3), which are considered vulnerable locations of voltage fluctuation. In addition, significant voltage deviation occurs along the tail part of the main feeder circuit line (bus $6-18$).

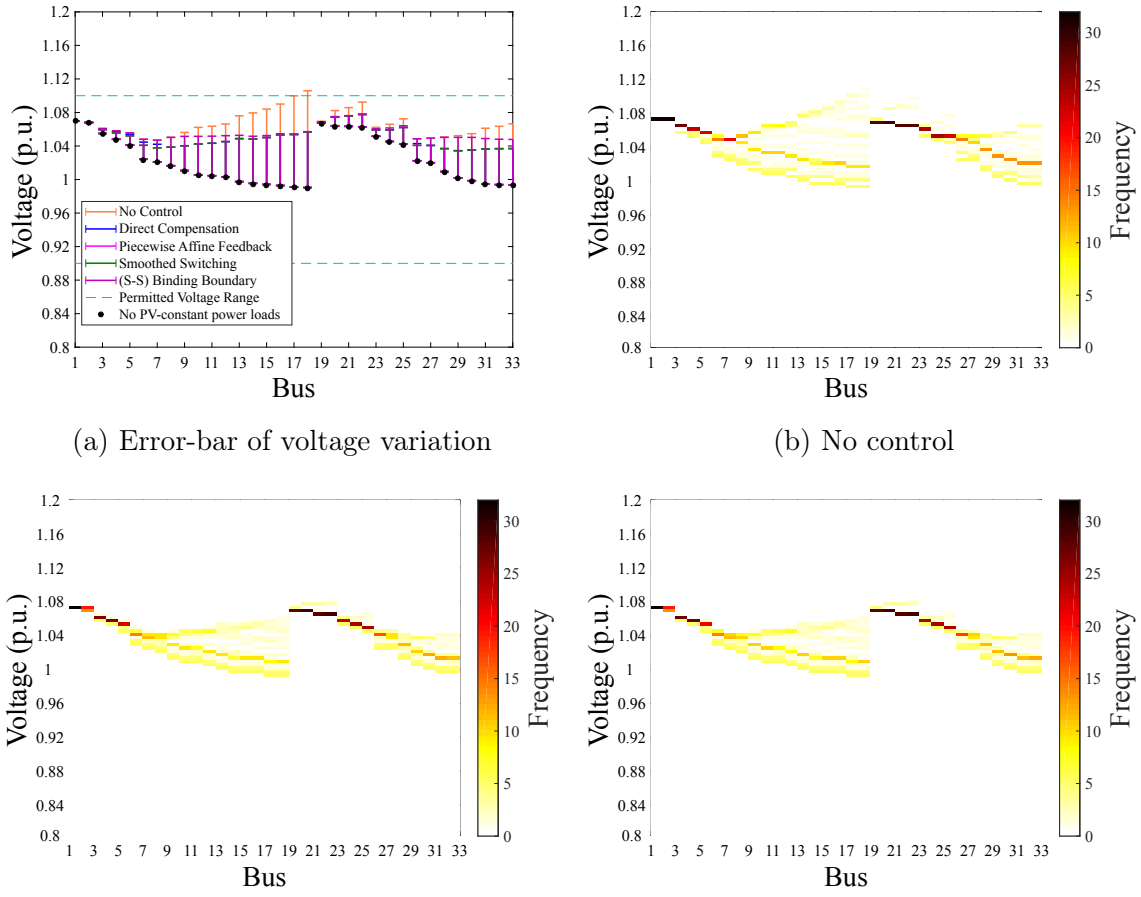

(a) Error-bar of voltage variation

(b) No control

(c) Direct compensation control

(d) Piecewise feedback Affine

Figure 4.6: 1 PV: Voltage variation and its deviation with respect to PV allocation

Random allocation of few PV generators is also conducted with 6 PV generators. The net real power generation of PV is set the same as 50% of net real power demand. Combination of PV allocation patterns grows dramatically, the associated voltage deviation results are shown in Figure 4.7. As power generation of single PV in 6 PV case is smaller than the 1 PV case, voltage deviation ranges are shortened comparing with those in the 1 PV generator case. However, decentralized reactive

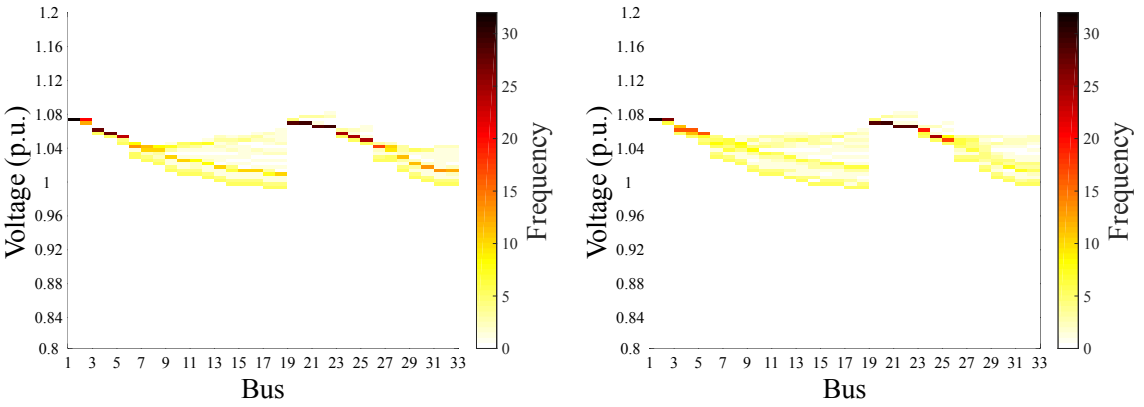

(e) Smoothed switching (f) S-S with binding boundary control

Figure 4.6: (Continued)

power control schemes are still insufficient to suppress voltage deviation with respect to all combination of PV allocation patterns. Color-bar figures in Figure 4.7 shows the same tendency as the 1 PV case, where the connecting buses of circuit lines have high frequency of voltage deviations.

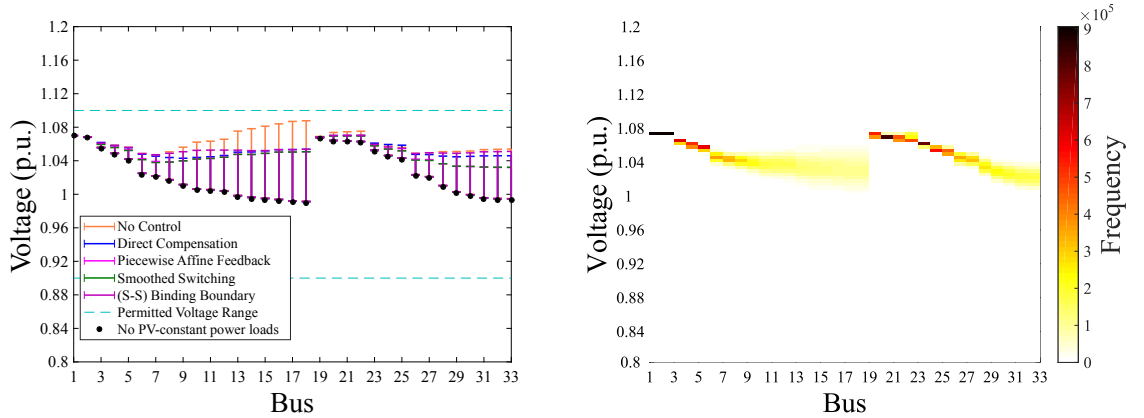

(a) Error-bar of voltage variation (b) No control

Figure 4.7: 6 PV: Voltage variation and its deviation with respect to PV allocation

Power loss in each controller is also estimated for the 1 and 6 PV cases. Energy loss along the circuit line is calculated with the following equation:

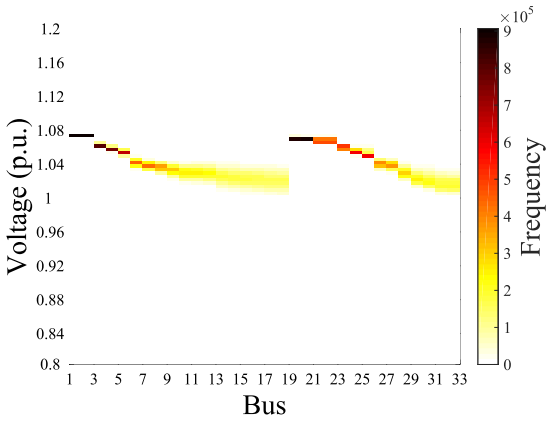

(c) Direct compensation control

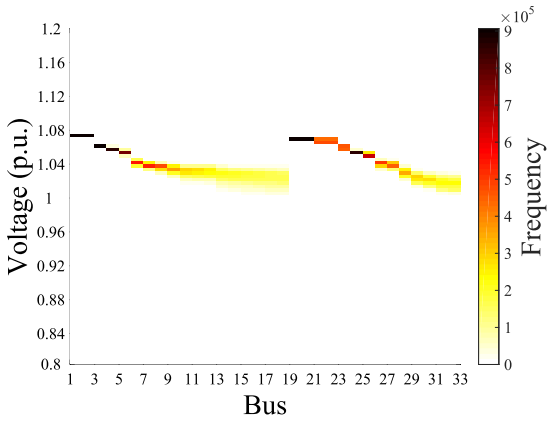

(d) Piecewise feedback Affine

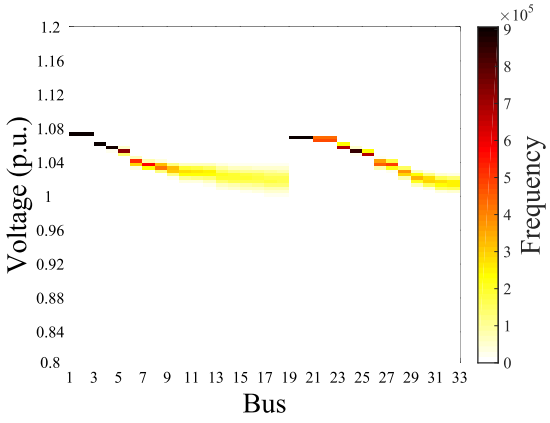

(e) Smoothed switching

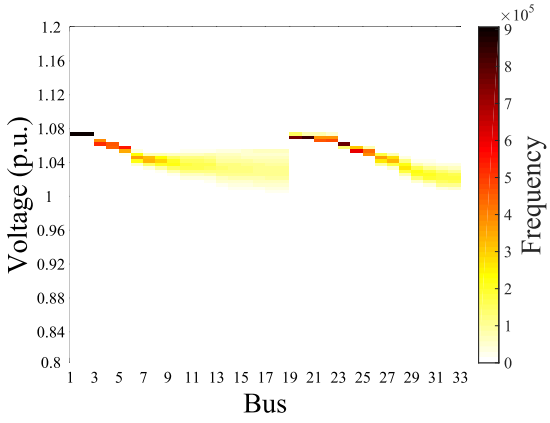

(f) S-S with binding boundary control

Figure 4.7: (Continued)

$$\sum_{j=1}^{n} r_j \frac{(P_j^2 + Q_j^2)}{V_j^2} \tag{4.6}$$

Power loss with respect to PV allocation patterns in each control scheme is demonstrated with histograms shown in Figure 4.8. Frequency axis shown in Fig. 4.8 means the occurrence of situation. Smoothed switching with binding boundary case has better results compared to other controllers. Also, the smoothed switching with binding boundary method results in large range of changes in power loss with respect to PV allocation patterns in 6 PV case of Figure 4.8b.

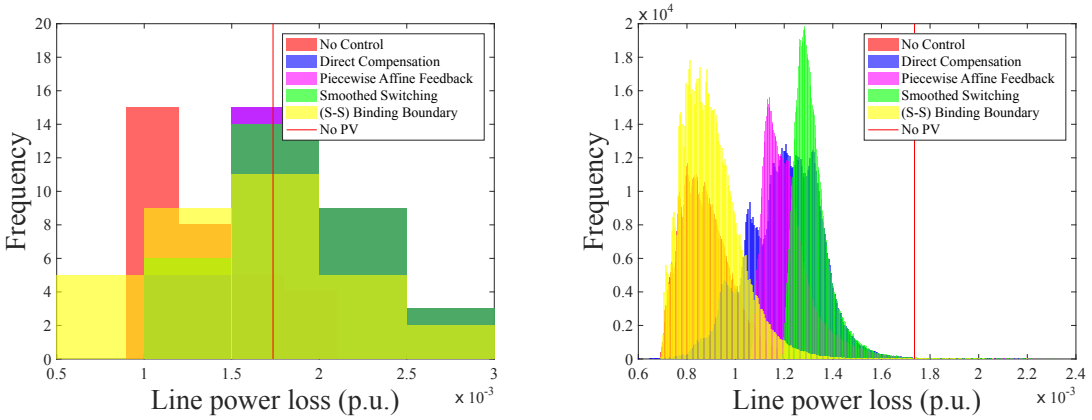

(a) 1 PV generators (b) 6 PV generators

Figure 4.8: Power losses along circuit line

From the general evaluation of five controllers, inverter reactive power control shows effectiveness in voltage regulation during large and random PV penetration, though the reactive power capability of inverter limits the control performance of the controllers. From the voltage stability point of view, control performance is insufficient, when managing reactive power injection of inverter based on the local voltage information. Moreover, more PV generators with the same

4.3.2 Uniform distribution of numerous PV generators

Other than integrating few number of PV generators, net PV generation is uniformly distributed among all consumer buses in this case: First, set power generation of one PV as 2kW, apparent power of PV as 2.2kVA. Second, fixed the net real power generation of PV as 50% of consumer real power demand; Third, divide the net power generation of PV by 2kW into large number of PV generators; Fourth, uniformly distribute these PV generators among consumer buses. This process demonstrated above is sampling for 10^5 times, which aims to investigate voltage variation with respect to PV allocation patterns.

The associated deviation range of voltage is shown in Figure 4.9a. Voltage rises at each bus for all sampling of PV distribution, rather than varying in a large range. In addition, control performances differs with respect to controllers. The piecewise affine feedback and smoothed switching with binding boundary controllers show better control performance than the other two controllers. However, control performance of basic control schemes are still insufficient in the case of uniform distribution of PV generators. The frequencies of voltage deviations with respect to random PV

integration are shown in Figure 4.9, where inverter controllers are able to change the voltage variation frequencies slightly with different control parameters.

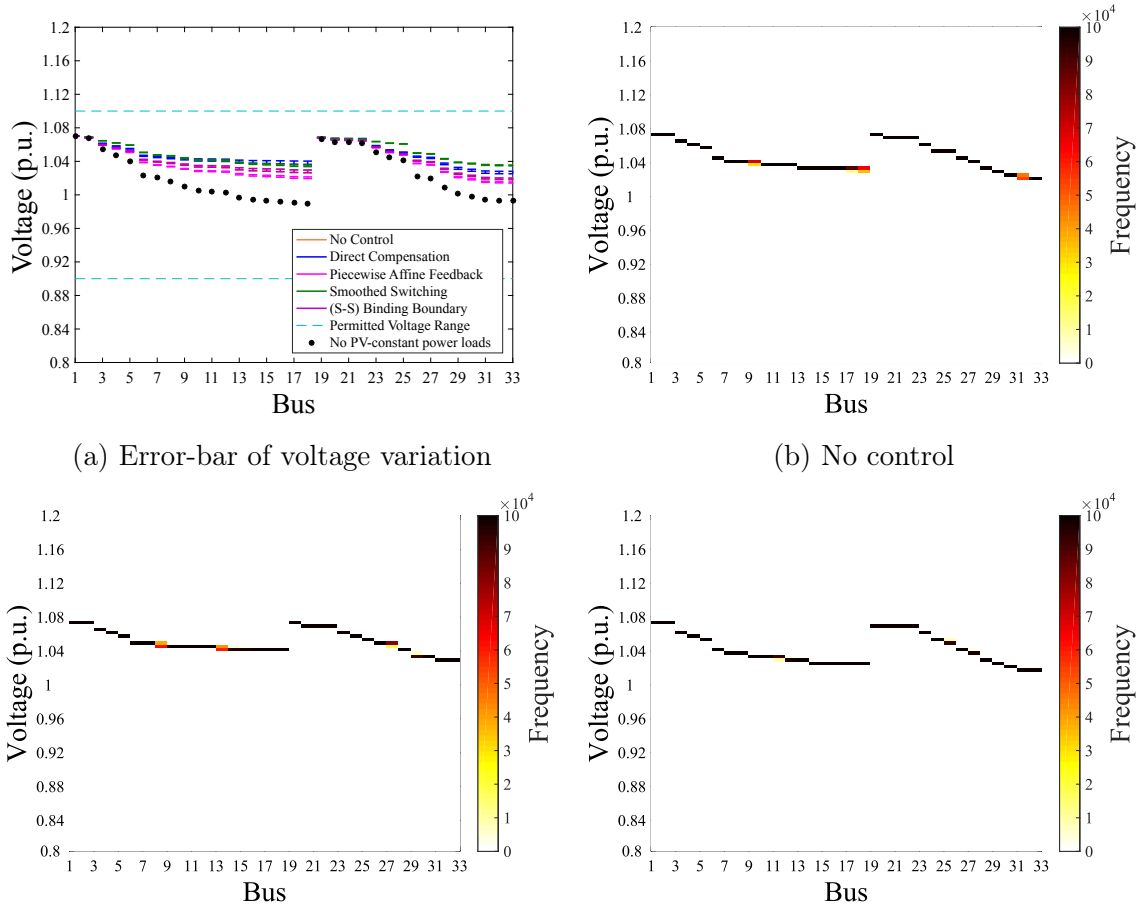

(a) Error-bar of voltage variation

(b) No control

(c) Direct compensation control

(d) Piecewise feedback Affine

Figure 4.9: Uniform distribution of numerous PV generators

4.4 Clustering analysis

When large number of PV generators randomly integrate with power system, combination of all possible PV allocation patterns formulates large data set that becomes difficult or even impossible to analyze. To reduce the computational load, Pregelj *et al.* has used k-Means clustering method to investigate the voltage profiles under various load conditions and uncertain power output of distributed generators [68]. However, k-Means method represents each partitioned cluster with a mean value

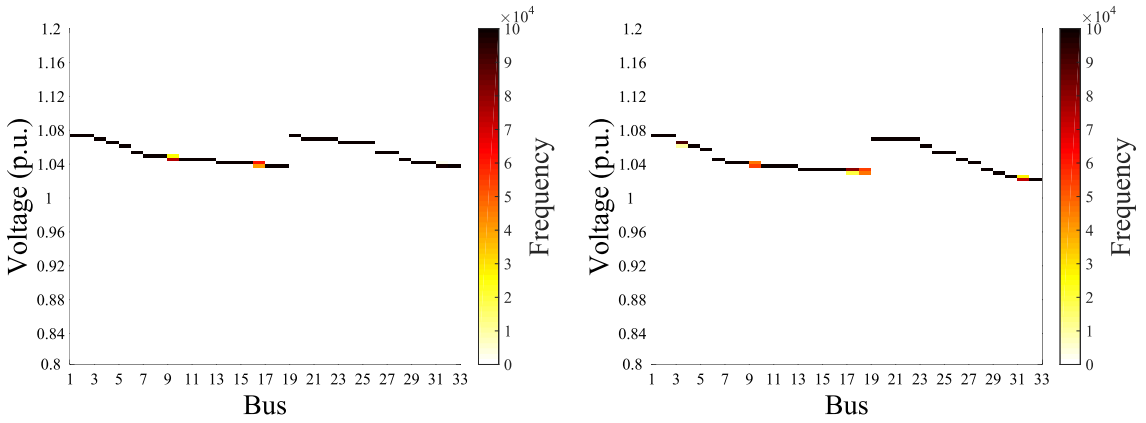

(e) Smoothed switching (f) S-S with binding boundary control

Figure 4.9: (Continued)

of its members, which is not suitable to analyze representative allocation pattern of PV generators in each partitioned cluster. This study considers to choose k-Medoids clustering method to investigate the large data set of voltage profiles under various PV allocation patterns, which contributes to select representative PV allocation pattern for members in one cluster [44].

4.4.1 Clustering method

Assume there is a data set X, k-Medoids clustering algorithm divides X into a pre-determined number of clusters, and selects one representative point of each cluster among X. The representative point of each cluster is called medoid. Let η be the set of medoids for all clusters, I_η be the set of indices of medoids in X. Besides medoid of each cluster, membership of a point included in a cluster is expressed with equation below:

$$\mu_{ij} = \begin{cases} 1, & \text{if } d(x_i, x_j) = \min_{q \in I_\eta} d(x_i, x_q) \\ 0, & \text{otherwise} \end{cases} \tag{4.7}$$

where μ_{ij} denotes the membership of point x_i with respect to each medoid x_q in η. When x_i lies close enough to its medoid, u_{ij} is set to 1, otherwise, u_{ij} is set to 0. Quality of the clustering with a pre-determined number of clusters is evaluated by the following cost function:

$$J(\Theta, U) = \sum_{i \in I_{X-\Theta}} \sum_{j \in I_{\Theta}} \mu_{ij} d(x_i, x_j) \tag{4.8}$$

Minimize the cost function Equation (4.8) to obtain the optimal set of medoids η, and their members. Similar voltage profiles with respect to various PV allocation patterns are partitioned into each cluster. These analysis technique is well suitable for analysis of large data set of power flows, under large and random PV allocations.

4.4.2 Results of clustering

Random allocation of 6 PV generators is chosen to demonstrate the analysis results with k-Medoids clustering method.The number of clusters is pre-determined as 1000. X is set as voltage profiles with respect to all combination of PV allocations. Each cluster collects similar voltage profiles under various PV allocation patterns. Then, X is reduced into 1000 small groups of data, which simplifies the analysis PV allocation patterns with respect to voltage deviation. Voltage profiles in direct compensation method are taken as example to show the analysis process of clustering method, the associated clustering results are shown in Figure 4.10.

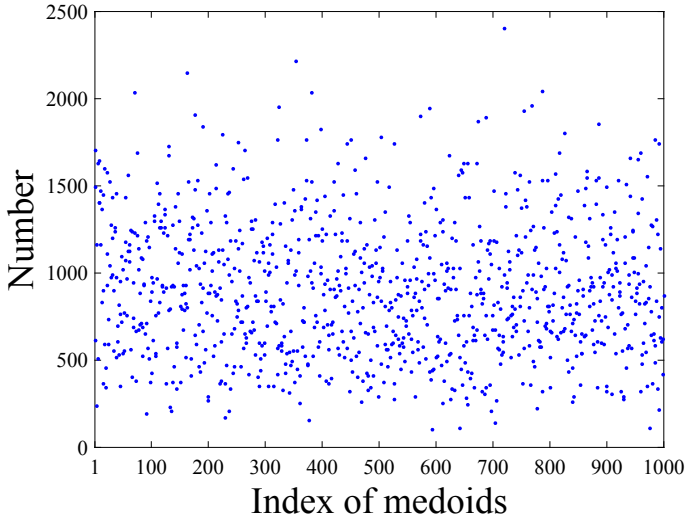

(a) Number of members in each cluster

Figure 4.10: Clustering analysis of sample case: Direct compensation control

The number of points in each cluster is shown in Figure 4.10a. Two clusters are chosen from the 1000 clusters to analyze the variation range of voltage and the PV allocation patterns. The two clusters are index number 992 and 721, where index number of cluster No. 992 indicate the worst voltage deviation at bus 18, and holds a number of 211 points of voltage profiles. On the other hand, index number of cluster No. 721 has the largest number of members, 2403. The points of voltage profiles in each cluster is a subset of X, which formulate variation range of voltage in each cluster. Voltage variation ranges of cluster No. 992 and 721 are shown in Figure 4.10b, where the green square and red circle denote voltage profile of medoid No. 992 and 721 respectively, and their associated PV allocation patterns are shown with upward and downward triangles. In Figure 4.10b, cluster No. 992 with small group of members result in larger voltage variation range than that of cluster No. 721. As only a small number of the PV allocation patterns results in severe voltage deviation, which would simplify the analysis of severe voltage fluctuation due to certain PV allocation patterns. The comparison of PV siting frequency in each cluster is plotted in Figure 4.10c. For cluster No. 721, PV generators tend to uniformly distributed among circuit lines. However, PV allocation patterns of cluster No. 992 tend to concentrate on the tail part of feeder circuit line, which result in severe voltage deviation at bus 18. Through the process demonstrated above, the PV allocation patterns would be investigated for each cluster. The analysis results of voltage stability with respect to PV allocation patterns, indicate that certain dangerous PV siting patterns might harm voltage stability severely even with same PV generation.

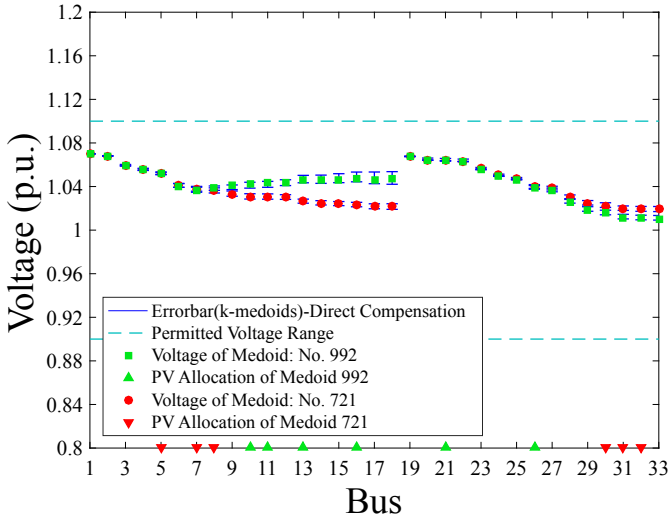

(b) Range of voltage variation in cluster No. 721, No. 922

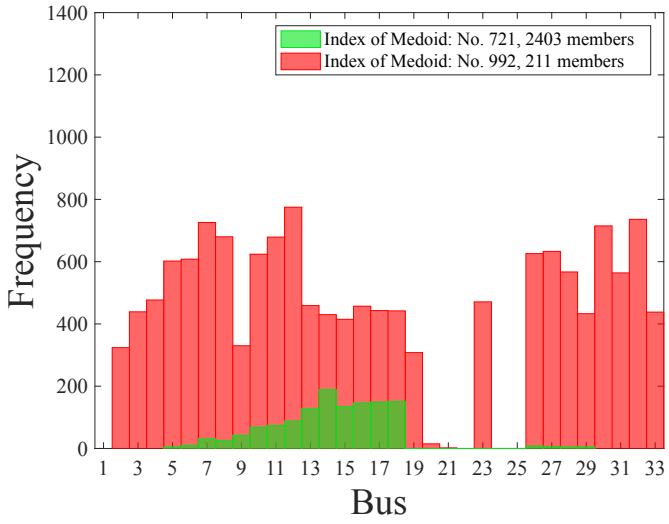

(c) Frequency of PV allocation at each bus in cluster No. 721, No. 922

Figure 4.10: (Continued)

4.5 Summary

Statistical analyses of voltage stability are conducted in power system under large and random PV allocations. Decentralized reactive power control schemes are applied on PV inverters. Allocation patterns of PV are sorted into cases: one is random distribution of small number of PV generators, the other is uniform distribution of large number of PV generators. Radial distribution system of IEEE 33-bus power system is chosen as benchmark example to investigate the voltage stability with respect to various PV allocation patterns and inverter controllers. The associated analysis results show that severe voltage deviation commonly occurs around the tail part of circuit lines. In addition, the connecting parts of system tend to be vulnerable buses of voltage stability with respect to PV integration. Furthermore, decentralized inverter controllers are insufficient to suppress voltage deviation with respect to various PV allocation patterns. When data set of voltage profiles grow with respect to the increase of PV allocation patterns, k-Medoids clustering method is considered to partition the data set of voltage variation. k-Medoids method selects representative point of each cluster from the original data set and contributes to investigate PV allocation patterns with similar voltage deviations. Voltage profiles due to random PV integration from the direct compensation method are utilized to demonstrate the clustering results. Two clusters in the clustering analysis are chosen to compare the characteristics of voltage variation and PV allocation patterns in each cluster. High voltage deviation occurs when assignment of PV generators concentrate on the tail part of feeder circuit line. Although the clustering analyses of sample cases indicate that the k-Medoids clustering method partitions the data set of voltage profiles with respect to random PV integration successfully, the optimal number of clusters for a data set is left for further investigation.

Chapter 5

Efficient reactive power control using sparse optimization

The basic control schemes demonstrated in Chapter 4 were induced as decentralized controllers in the radial distribution system, the performance of voltage regulation varied with respect to different PV allocation patterns. To overcome this drawback, an efficient reactive power control method is proposed with the aid of sparse optimization technique. To be clear, this sparse optimization technique is applied on the meshed power system, as it is a general representative of power system. First, nonlinear power flow equations of power system is linearized. Under the current operating point, the relation between voltage magnitude change and inverter reactive power change is derived from the linearized power flow equations in Section 5.1. Then, the voltage regulation problem is formulated as to minimize the regulation error subject to the constraint of inverter power capability, where two types of penalty functions are analyzed: one is a standard constrained least-square method demonstrated in Section 5.2, the other is called constrained least absolute shrinkage and selection operator (LASSO) introduced in section 5.3, the constrained LASSO method contributes to select essential PV inverters for voltage regulation. The effectiveness of the proposal on voltage regulation is analyzed on 39-bus and 57-bus power systems in Section 5.4.

5.1 Linearized model

A linear relation between voltage magnitude change and reactive power change is derived from the nonlinear power flow equations in Equation (3.2). Take its gradient at the operating point to realize the linearization, which gives [69]:

$$\begin{bmatrix}\Delta P\\ \Delta Q\end{bmatrix} = -J \cdot \begin{bmatrix}\Delta\Theta\\ \Delta V\end{bmatrix} \tag{5.1}$$

where J is Jacobian matrix, and composed of partial derivatives of Equation (3.2) with respect to vector of voltage angle Θ and voltage magnitude V as follows:

$$J = \begin{bmatrix}J_{11} & J_{12}\\ J_{21} & J_{22}\end{bmatrix} := \begin{bmatrix}\frac{\partial\Delta P}{\partial\Theta} & \frac{\partial\Delta Q}{\partial\Theta}\\ \frac{\partial\Delta P}{\partial V} & \frac{\partial\Delta Q}{\partial V}\end{bmatrix} \tag{5.2}$$

At the current operating point, real power demand of consumer buses, real power generation of PV, and real power generation of generator buses are assumed to be unchanged, which gives the following constraint:

$$\Delta P_f = 0, \quad \forall f \in \mathcal{I}_d \cup \mathcal{I}_g \tag{5.3}$$

Substitute Equation (5.2) and Equation (5.3) for Equation (5.1), the relation between reactive power change and voltage magnitude change is derived [49]:

$$\begin{aligned}\Delta Q &= [J_{21}J_{11}^{-1}J_{12} - J_{22}]\Delta V\\ &= J_{\mathrm{R}}\Delta V\end{aligned} \tag{5.4}$$

where $J_{\mathrm{R}} = [J_{21}J_{11}^{-1}J_{12} - J_{22}]$.

In addition, reactive power demand of non-PV integrated consumer buses remains its demand at the operating point, thus, their reactive power changes would also be zero. The constraint is described as:

$$\Delta Q_l = 0, \quad \forall l \in \mathcal{I}_d \cap \mathcal{H} \tag{5.5}$$

Rearrange the sequence of Equation (5.4) by non-PV and PV-enabled consumer buses respectively, and reformulate it as [26]:

$$\begin{bmatrix}0\\ \Delta Q_{\mathrm{PV}}\end{bmatrix} = \begin{bmatrix}B_{11} & B_{12}\\ B_{21} & B_{22}\end{bmatrix} \cdot \begin{bmatrix}\Delta V_{\mathrm{L}}\\ \Delta V_{\mathrm{PV}}\end{bmatrix} = B \cdot \begin{bmatrix}\Delta V_{\mathrm{L}}\\ \Delta V_{\mathrm{PV}}\end{bmatrix} \tag{5.6}$$

where ΔV_{L} and ΔV_{PV} denote vectors of voltage magnitude change at non-PV and PV-enabled consumer buses respectively; ΔQ_{PV} is vector of reactive power change at

PV-enabled consumer buses; matrix J_{R} is reformulated into matrix B. With Equation (5.6), relation between ΔQ_{PV} and ΔV_{PV} is obtained:

$$\begin{aligned} \Delta Q_{\mathrm{PV}} &= (B_{22} - B_{21}B_{11}^{-1}B_{12})\Delta V_{\mathrm{PV}} \\ &= B_{\mathrm{R}}\Delta V_{\mathrm{PV}} \end{aligned} \tag{5.7}$$

where $B_{\mathrm{R}} = [B_{22} - B_{21}B_{11}^{-1}B_{12}]$. So voltage change can be expressed as:

$$\Delta V_{\mathrm{PV}} = B_{\mathrm{R}}^{-1}\Delta Q_{\mathrm{PV}} \tag{5.8}$$

Note the dimensions of vectors with subscript of block capital PV are different from that of lower case pv, as the dimensions of their representing vectors are different. Based on Equation (5.8), control problem is formulated in Section 5.2 and 5.3.

5.2 Constrained least-square method

To suppress voltage change to a pre-designed response ΔV_{PV}, optimal reactive power change can be calculated with the linear model of Equation (5.8) using constrained least-square method, which searches the best fit of reactive power change ΔQ_{PV}, that minimizes the sum of the squared residuals of Equation (5.8). As the ΔQ_{PV} is constrained by inverter power capability, the optimization problem is formulated with a constrained least-square method:

$$\begin{aligned} &\min_{\Delta Q_{\mathrm{PV}}} \frac{1}{2} \parallel \Delta V_{\mathrm{PV}} - B_{\mathrm{R}}^{-1}\Delta Q_{\mathrm{PV}} \parallel_2^2 \\ &\text{subject to: } |\Delta Q_{\mathrm{PV},k}| \leq \sqrt{S_{\mathrm{pv}}^2 - P_{\mathrm{pv},k}^2}, \quad \forall k \in \mathcal{H} \end{aligned} \tag{5.9}$$

where S_{pv} denotes the inverter apparent power capability, $P_{\mathrm{pv},k}$ is the real power generation from PV at k-th bus.

However, the author wonders if the solution to the constrained leas-square method can be shrunk further. For example, reduce the solutions with all non-zero entries to only a few representative ones. The idea motivates the author add ℓ^1-norm penalty to ΔQ_{PV}, and adopt the constrained LASSO method to formulate the optimization problem.

5.3 Constrained least absolute shrinkage and selection operator method

A linear least-square regression problem is often described as:

$$\min_x \frac{1}{2} \parallel C - Dx \parallel_2^2 \tag{5.10}$$

where x denotes a vector of regression coefficients, D is a pre-designed matrix of predictor variables, and C is a vector of response variables. Let $\hat{x}$ be the solution of Equation (5.10), which leads to:

$$\hat{x} = (D^{\mathrm{T}}D)^{-1}D^{\mathrm{T}}C \tag{5.11}$$

The least absolute shrinkage and selection operator (LASSO) adds a ℓ^1-norm penalty to its regression coefficients as $\parallel x \parallel_1$, which leads to equation [52,53]:

$$\min_x \frac{1}{2} \parallel C - Dx \parallel_2^2 + \rho \parallel x \parallel_1 \tag{5.12}$$

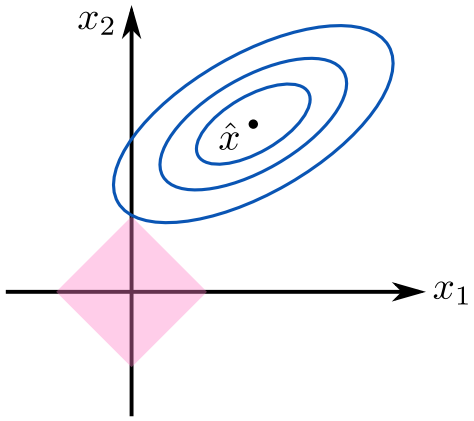

Figure 5.1: Illustration of LASSO

Take two dimension of x as an example, Figure 5.1 shows an illustration of LASSO optimization. Assume x only have two parameters, which consists of x_1 and x_2. The summed square of residuals with respect to an estimate has elliptical contour that centering at $\hat{x}$ [70], which is plotted with blue lines. Constant tuning parameter ρ

and ℓ^1-norm penalty in Equation (5.12) gives constraint $|x_1| + |x_2| \leq t$, where t is a constant tuning parameter that can be expressed with ρ. Region of this constraint is illustrated with pink diamond shape in Figure 5.1. Solution of LASSO is the first point on contour line that hits with the constraint region. As diamond shape has corners, if the solution happens to be at the corner like Figure 5.1, then one of the coefficient estimates equals to zero. When the dimension of x is larger than 2, corners of the constraint region will increase. Therefore, there will be more chance of coefficient estimates equal to zero. The ℓ^1-norm penalty on x contributes to shrink some of the estimated coefficients towards zero.

The LASSO method works in the desired feature of the formulated optimization problem. Apply the LASSO method on the linearized model, which obtains:

$$\min_{\Delta Q_{\mathrm{PV}}} \frac{1}{2} \parallel \Delta V_{\mathrm{PV}} - B_{\mathrm{R}}^{-1} \Delta Q_{\mathrm{PV}} \parallel_2^2 + \beta \parallel \Delta Q_{\mathrm{PV}} \parallel_1 \tag{5.13}$$

Since reactive power capability is limited by Equation (2.4), the LASSO should subject to the constraint as in Equation (5.9). Constrained LASSO method developed by [50,51] allows prior constraints to be added on the regression coefficients, which would suit the optimization problem here. The formulation is demonstrated below:

$$\begin{aligned} &\min_{\Delta Q_{\mathrm{PV}}} \frac{1}{2} \parallel \Delta V_{\mathrm{PV}} - B_{\mathrm{R}}^{-1} \Delta Q_{\mathrm{PV}} \parallel_2^2 + \beta \parallel \Delta Q_{\mathrm{PV}} \parallel_1 \\ &\text{subject to: } |\Delta Q_{\mathrm{PV},k}| \leq \sqrt{S_{\mathrm{pv}}^2 - P_{\mathrm{pv},k}^2}, \quad \forall k \in \mathcal{H} \end{aligned} \tag{5.14}$$

where β is the tuning parameter to determine the shrinkage on ΔQ_{PV} and control the essential required number of PV inverters to regulate voltage deviation. The effectiveness of the constrained LASSO method on voltage regulation in PV integrated power systems is analyzed under various power generation and allocation patterns of PV.

5.4 Benchmark analysis of the proposed method

As mentioned previously, two power systems are taken as benchmark examples to analyze the performance of the optimization techniques, which are IEEE 39-bus and 57-bus power systems. The 39-bus power system is a general representative of New England power system, with 10 generator buses, 29 consumer buses, and 46 branches [71]. The 57-bus power system represents a portion of American power system during

1960's, with 7 generator buses, 50 consumer buses, and 80 branches [72]. Both total and individual consumer demand of 39-bus power system are larger than 57-bus power system. Performances of the control schemes on both power systems are expected not influenced by their different network configurations and initial system parameters. The comparison of the analysis results turns out in similar tendencies of effects on voltage regulation. Thus, one of the two system is mainly chosen to demonstrated the results, where 39-bus power system is used here. The network configuration of this system is shown in Figure 5.2, base voltage and power are 345kV and 100MVA respectively.. The consumer demand of each bus and branch data are listed in Table 5.1, the generator data is listed in Table 5.2. As the shunt elements of buses are zero, which are not listed here. In the absence of PV generators, power flow is calculated with Equation (3.2), the associated power flow data and voltage profile are plotted in Figure 5.3a and Figure 5.3b. Buses from 1 to 29 are consumer buses, where the blue and yellow bars indicate real and reactive power demand respectively. Buses from 30 to 39 are generator buses, red and black bars are real and reactive power generation. Voltage profile would change while PV generators connected with the power system, and their impacts are analyzed in the following sections.

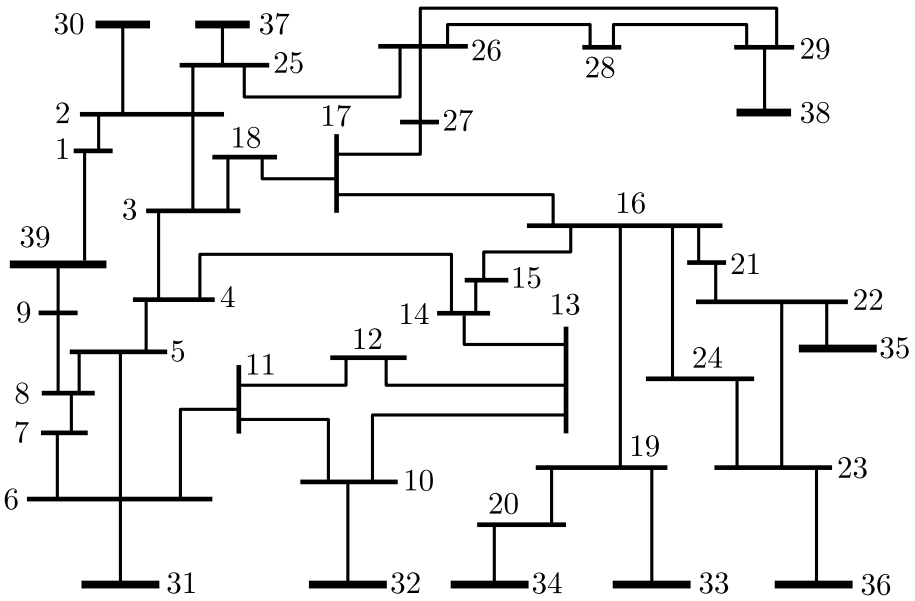

Figure 5.2: Network configuration of IEEE 39-bus power system

Table 5.1: Bus and branch data in 39-bus power system

Bus data			**Branch data**			
Bus	P_d (MW)	Q_d (MVAr)	From	To	r (Ω)	x (Ω)
1	97.6	44.2	1	2	0.0035	0.0411
2	0	0	1	39	0.001	0.025
3	322	2.4	2	3	0.0013	0.0151
4	500	184	2	25	0.007	0.0086
5	0	0	2	30	0	0.0181
6	0	0	3	4	0.0013	0.0213
7	233.8	84	3	18	0.0011	0.0133
8	522	176.6	4	5	0.0008	0.0128
9	6.5	-66.6	4	14	0.0008	0.0129
10	0	0	5	6	0.0002	0.0026
11	0	0	5	8	0.0008	0.0112
12	8.53	88	6	7	0.0006	0.0092
13	0	0	6	11	0.0007	0.0082
14	0	0	6	31	0	0.025
15	320	153	7	8	0.0004	0.0046
16	329	32.3	8	9	0.0023	0.0363
17	0	0	9	39	0.001	0.025
18	158	30	10	11	0.0004	0.0043
19	0	0	10	32	0	0.02
20	680	103	12	11	0.0016	0.0435
21	274	115	12	13	0.0016	0.0435
22	0	0	13	14	0.0009	0.0101
23	247.5	84.6	14	15	0.0018	0.0217
24	308.6	-92.2	15	16	0.0009	0.0094
25	224	47.2	16	17	0.0007	0.0089
26	139	17	16	19	0.0016	0.0195
27	281	75.5	16	21	0.0008	0.0135
28	206	27.6	16	24	0.0003	0.0059
29	283.5	26.9	17	18	0.0007	0.0082
30	0	0	17	27	0.0013	0.0173
31	9.2	4.6	19	20	0.0007	0.0138
32	0	0	19	33	0.0007	0.0142
33	0	0	20	34	0.0009	0.018
34	0	0	21	22	0.0008	0.014

(Continued on next page)

Table 5.1: (Continued)

Bus data			**Branch data**			
Bus	P_g (MW)	Q_g (MVAr)	From	To	r (p.u.)	x (p.u.)
35	0	0	22	23	0.0006	0.0096
36	0	0	22	35	0	0.0143
37	0	0	23	24	0.0022	0.035
38	0	0	23	36	0.0005	0.0272
39	1104	250	25	26	0.0032	0.0323
			25	37	0.0006	0.0232
			26	27	0.0014	0.0147
			26	28	0.0043	0.0474
			26	29	0.0057	0.0625
			28	29	0.0014	0.0151
			29	38	0.0008	0.0156

Table 5.2: Generator data in 39-bus power system

Bus	P_g (MW)	V_g (p.u.)	Bus	P_g (MW)	V_g (p.u.)
30	250	1.0499	31	677.871	0.982
32	650	0.9841	33	632	0.9972
34	508	1.0123	35	650	1.0494
36	560	1.0636	37	540	1.0275
38	830	1.0265	39	1000	1.03

5.4.1 Performance evaluation indices

Three indices are introduced–MSE, VSM and RP to evaluate the performance of the proposed control schemes. MSE stands for the mean square error of voltage regulation, which measures the precision of voltage control; VSM denotes the gross voltage stability margin that indicates the capability of power injection from PV; RP calculates the net absolute reactive power generation, which is for the control cost of inverter reactive power. The detail explanation of each indicator is demonstrated below:

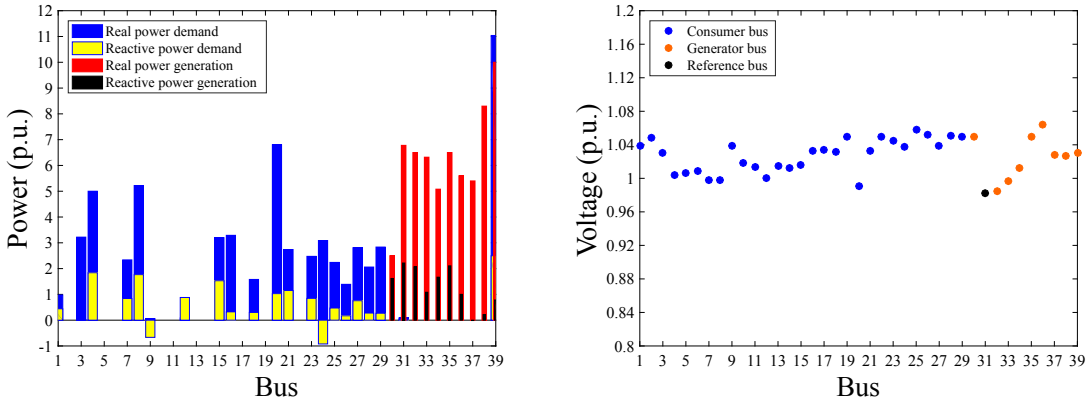

(a) Power flow data (b) Voltage profile without PV generation

Figure 5.3: IEEE 39-bus power system

Mean Square Error of Voltage Regulation

The value of MSE measures the achievement of voltage regulation, V_{ref} denotes the vector of reference voltage, let V_{pv} be the resulting voltage with voltage regulation. MSE is computed as:

$$\text{MSE} = \frac{1}{n}\sum_{j=1}^{n}(V_{\text{pv},j} - V_{\text{ref},j})^2 \tag{5.15}$$

Performance of voltage regulation improves when the value of MSE decreases.

Voltage Stability Margin with Continuation Power Flow Method

The voltage stability margin is calculated with the assist of continuation power flow method. The continuation power flow, CPF for short, computes power flow solutions with respect to continuous power change [73,74], which solves the voltage stability limit (also named critical point) with respect to base (or initial) point and target (or operating) point of power flow. Let $X := (\Theta, V)$, $g(X)$ be the power flow at the base point, the CPF can be described as:

$$f(X, \lambda) = g(X) - \lambda b = 0 \tag{5.16}$$

where λ is a continuous parameter that features the continuous change of power in CPF; b is a vector of power transfer from the base point. PV generation changes the initial power injection of the bus, b can be composed as:

$$b = \begin{bmatrix} P_{\text{target}} - P_{\text{base}} \\ Q_{\text{target}} - Q_{\text{base}} \end{bmatrix} = \begin{bmatrix} P_g - (P_d - P_{\text{pv}}) - (P_g - P_d) \\ Q_g - (Q_d - Q_{\text{pv}}) - (Q_g - Q_d) \end{bmatrix} = \begin{bmatrix} P_{\text{pv}} \\ Q_{\text{pv}} \end{bmatrix} \tag{5.17}$$

where P_{base}, Q_{base} and P_{target}, Q_{target} are the vectors of initial power injection and PV-enabled power injection. With the power transfer rate b, critical point is computed by varying λ. The V-λ relation can be illustrated with a nose curve of voltage magnitude in Figure 5.4.

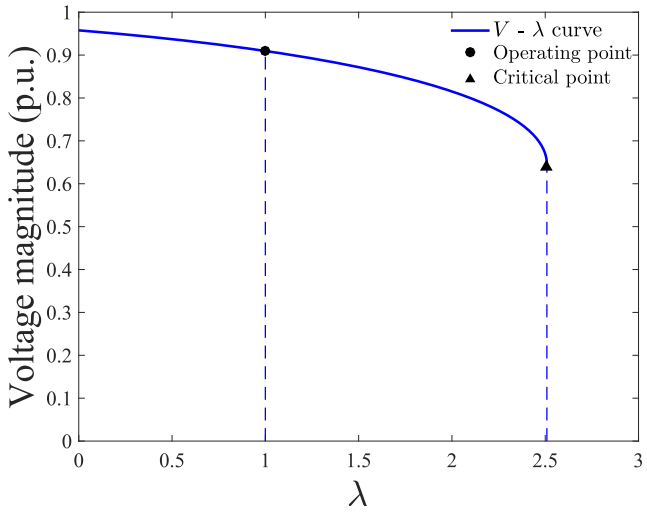

Figure 5.4: Nose curve of voltage magnitude at a bus

In this study, voltage stability margin of one bus is designed as the relative distance of λ between critical point and operating point. Let λ_{cp} and λ_{op} be the value of λ at critical point and operating point respectively in Figure 5.4, VSM is as follows:

$$\text{VSM} = \lambda_{\text{cp}} - \lambda_{\text{op}} \tag{5.18}$$

clearly from Equation (5.18), voltage stability improves when VSM increases.

Net Absolute Reactive Power Generation

Finally, the control cost is measured with the net absolute reactive power output from PV inverters, RP for short, which is computed as:

$$\mathrm{RP} = \sum_{k=1}^{K} |Q_{\mathrm{pv},k}|, \quad k \in \mathcal{H} \tag{5.19}$$

The decrease of RP is expected by using the constrained LASSO compared to the constrained least-square method, which indicates the the sparsity of the optimizing solution. This will be verified in the following description.

5.4.2 Analysis results

Analysis on the effectiveness of voltage regulation schemes was conducted by comparing differences among three cases in PV-enabled power system (without any reactive power control, with constrained least-square method and with constrained LASSO method). In addition, PV allocation are assigned in two patterns: one is to uniformly distribute PV generation to all the consumers, the other is to distribute PV generation proportional to the consumer demands. Note that, in the following analyses, the reference voltage V_{ref} is set as the voltage profile in the absence of PV generators.

Uniform Distribution of PV Generators

In this case, the nodal PV generation at one consumer bus is determined as follows: First, the total real power generation from PV is fixed as a portion of the total real power demand of consumer buses. Second, the total generation of PV is divided into small pieces, set the amount of a PV piece as 0.2 p.u.. Third, PV pieces is randomly assigned to consumer buses, under the rule of uniform probabilistic distribution. Finally, analyze the impacts of PV integration with the evaluation indices, and vary the share ratio of total PV generation from 5% to 45% to capture tendencies of changes in power system.

Under the distribution rule of PV generators demonstrated above, constrained least-square and LASSO method are applied in the 39-bus power system. The power generation of PV at each consumer bus, and the reactive power output in each controller can be expressed with a bar diagram, which contributes to roughly illustrate the difference in the two optimized solutions. Examples of PV power distribution and the resulting voltage profile are shown in Figure 5.5 in two cases, where the total PV generation is 10% and 30% of total real power demand respectively. In the figure of PV generation, the blue bars denotes the real power from PV, green bars represent the reactive power output from PV with constrained least-square method, and the magenta bars shows the reactive power output from PV with constrained LASSO

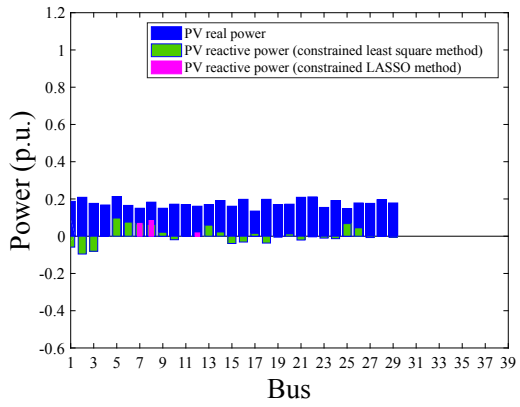

(a) Power distribution of PV in 10% case

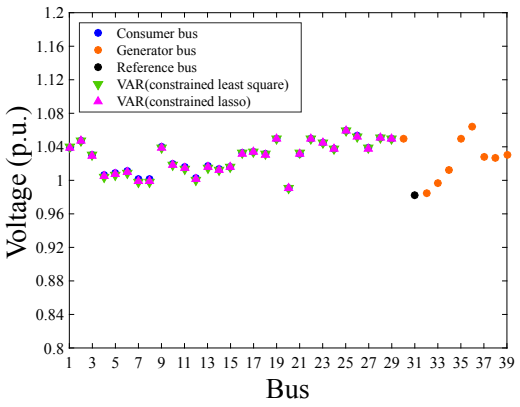

(b) Voltage profile of 10% case

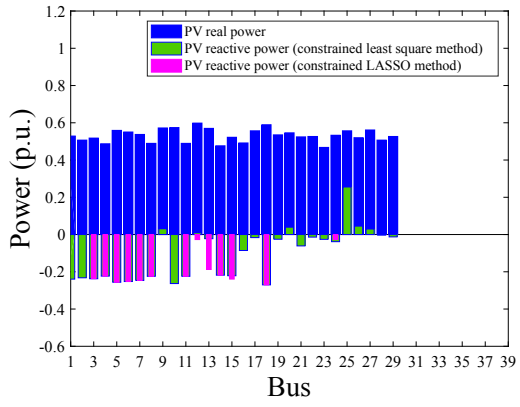

(c) Power distribution of PV in 30% case

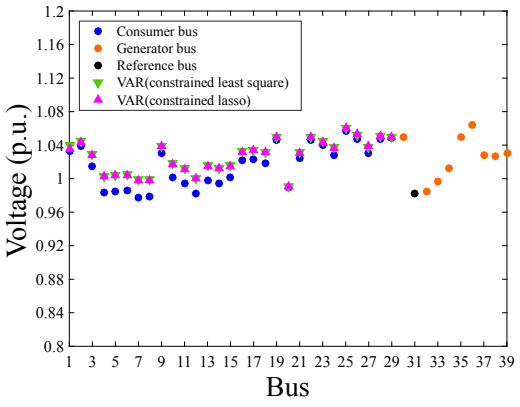

(d) Voltage profile of 30% case

Figure 5.5: PV power generation and voltage profile under uniform distribution of PV generators in 39-bus power system

method. In the figure of voltage profile, the colors are used to demonstrated the resulting voltage. Figure 5.7a and Figure 5.7b shows the power distribution of PV and the resulting voltage profile respectively. As the amount of PV generation was relatively low, voltage deviated slightly. The constrained LASSO controller selected only 3 PV inverters for voltage regulation, rather than choosing almost all PV inverters as the constrained least-square method. The same tendency occurs in the 30% case shown in Figure 5.7c and Figure 5.7d. Since the amount of PV generation increased, voltage severely deviated from the reference voltage at some buses. However, the constrained LASSO method succeeded in suppressing voltage variation with fewer reactive power than the other controller.

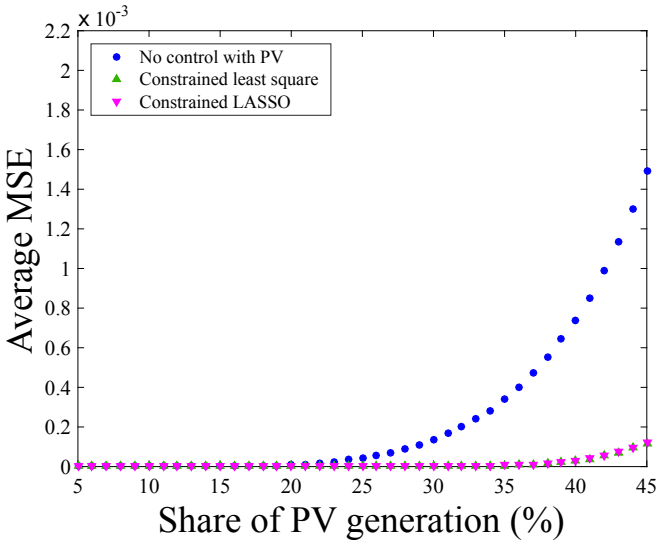

(a) Average MSE of voltage

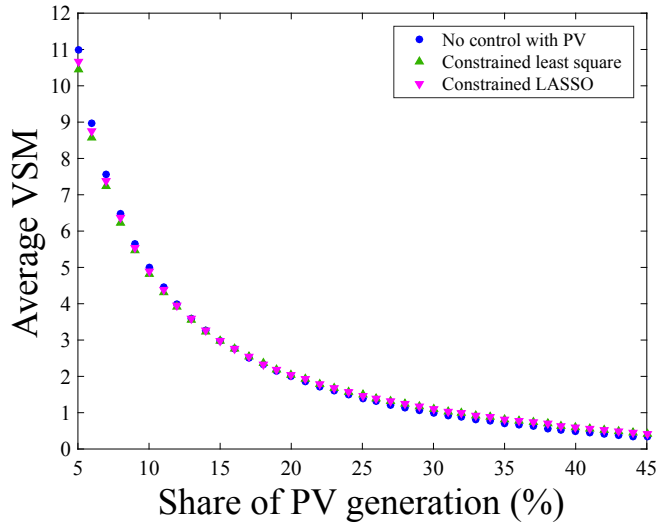

(b) Average VSM

Figure 5.6: Uniform distribution of PV generators in 39-bus power system

Let us go into a more detailed analysis. The share ratio of the net PV generation amount to the consumer demands was scanned, ranging from 5% to 45%. For each choice of the share ratio, random distributions were repeated 5 times. The averages of the corresponding indices (MSE, VSM and RP) over five trials are shown in Figure 5.6. The average MSE of voltage in Figure 5.6a shows that voltage magnitude varies severely

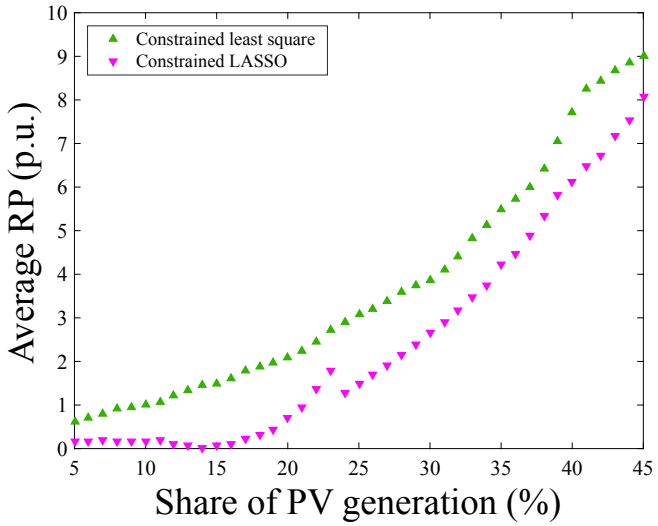

(c) Average RP

Figure 5.6: (Continued)

with respect to the increase of PV power integration when no voltage regulation is applied to the PV inverters. Meanwhile, the constrained least-square method and constrained LASSO method control voltage deviation effectively compared with the no control case. The average VSM in Figure 5.6b shows that the voltage stability of the 39-bus power system decreases with respect to the growth of PV generation, although the PV inverter reactive power control with the constrained least-square and constrained LASSO method results in the improvement of system voltage stability compared with the no control case. In addition, the results in Figure 5.6a,b explain that the constrained least-square method and constrained LASSO method show very similar effectiveness on voltage regulation. However, the net absolute reactive power generation from PV, with respect to the increasing PV power generation plotted in Figure 5.6c, shows that voltage regulation with the constrained LASSO method results in less reactive power generation from PV inverters than with the constrained least-square method. In other words, the constrained LASSO method succeeds in selecting the minimum required number of PV inverters to control voltage variation, while maintaining the same effectiveness on voltage regulation as the constrained least-square method.

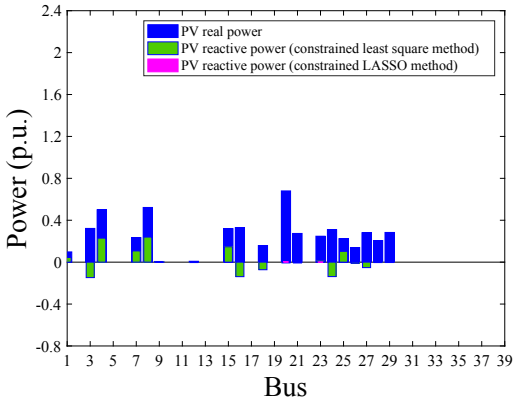

(a) Power distribution of PV in 10% case

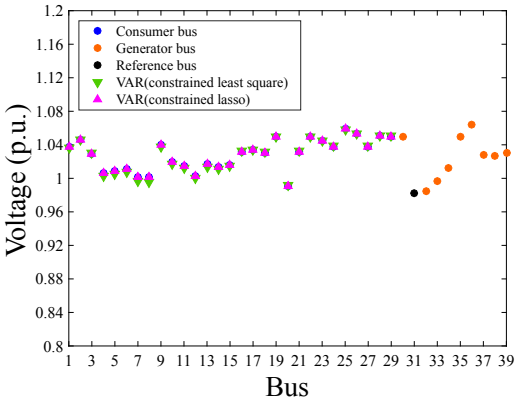

(b) Voltage profile of 10% case

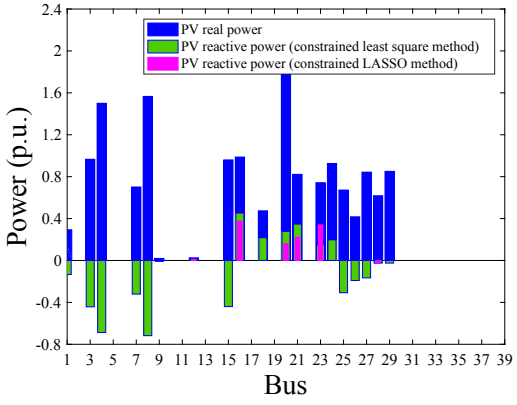

(c) Power distribution of PV in 30% case

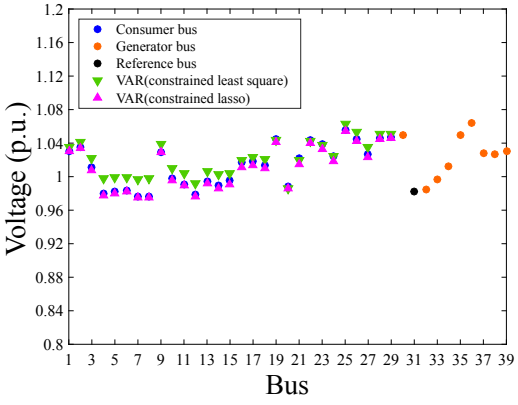

(d) Voltage profile of 30% case

Figure 5.7: PV power generation and voltage profile under on-demand distribution of PV generators in 39-bus power system

On-Demand Distribution of PV Generators

As opposed to the previous case, the non-uniform, weighted distribution of PV generators is considered in this case, which means that PV generators are only assigned to consumer buses with real power demand. In this case, the real power generation of PV at each bus is proportional to the consumer real power demand at the bus, where the PV/demand ratio is equal at each PV-enabled bus. The share ratio also ranges from 5% to 45%. The case is named as on-demand distribution of PV power generators here. Examples of 10% and 30% are shown in Figure 5.7. When power generation of PV is low as 10% of consumer demand, small voltage deviation occurs at each bus, minimal reactive power injections are required. However, when power

generation of PV rises to 30% of local consumer demand, the precision of voltage control differs between constrained least-square and LASSO method.

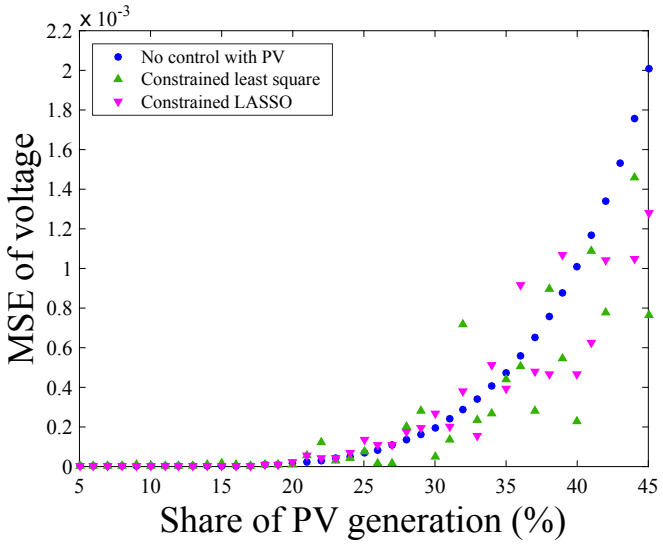

(a) MSE of voltage

Figure 5.8: On-demand distribution of PV power generators in 39-bus power system

The corresponding indices (MSE and RP) are shown in Figure 5.8. The net absolute reactive power generation from PV results in smaller value with the constrained LASSO method than with the constrained least-square method in Figure 5.8c. The constrained LASSO method shrinks the amount of inverter reactive power generation in the case of the on-demand distribution of PV generators. However, MSE of voltage varies severely with respect to the increase of PV real power generation in Figure 5.8a. The main reason is the validity of the linearization technique employed while formulating the control schemes. The linearization of power flow Equation (3.2) induces computing error to the voltage regulation process, and the reactive power constraint shown in Equation (5.5) accumulates this error when the number of PV-enabled buses declines. In the 39-bus power system, the number of PV-enabled consumer buses decreases in the on-demand case, since there is no power demand at some of the consumer buses. Consequently, the potential voltage regulation points of PV inverters became fewer, which impacted the precision of voltage regulation (MSE) to a certain extent. However, the authors consider that proper reference voltage design may suppress the computing error and improve the performance of MSE; a comprehensive study on this topic is left for future work.

The power loss of constrained least-square and LASSO are also plotted in Figure 5.9, which showed the power losses in both controllers are nearly identical to each other,

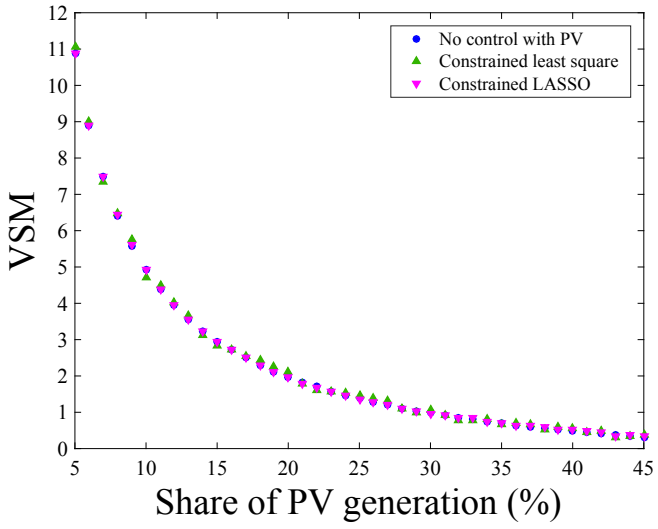

(b) VSM

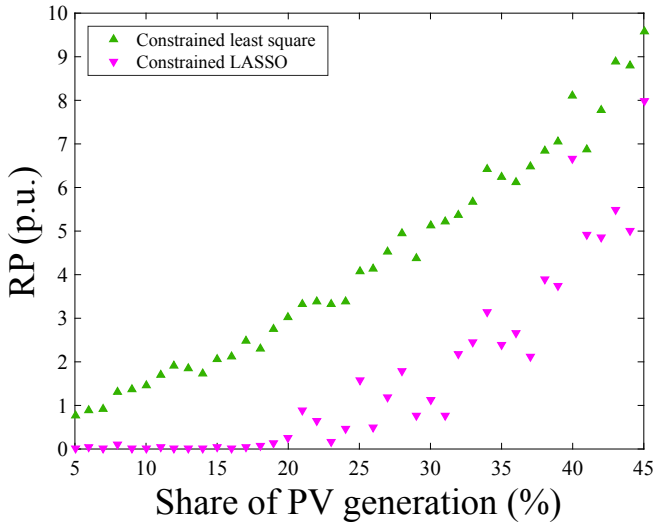

(c) RP

Figure 5.8: (Continued)

and the uniform distribution case results in less power losses than the on-demand distribution case.

Besides the 39-bus power system, IEEE 57-bus power system is also taken as benchmark example to evaluate the control performance of the proposed control method. Power flow data and voltage profile are shown in Figure 5.10 in the absence

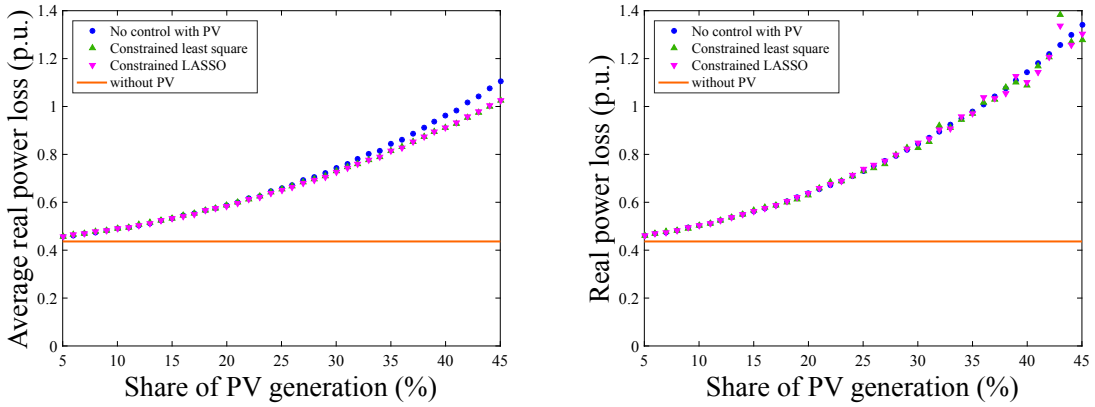

(a) Uniform distribution of PV generators (b) On-demand distribution of PV generators

Figure 5.9: Power losses in IEEE 39-bus power system

of PV generators. Same analyses demonstrated above are conducted on the 57-bus power system.

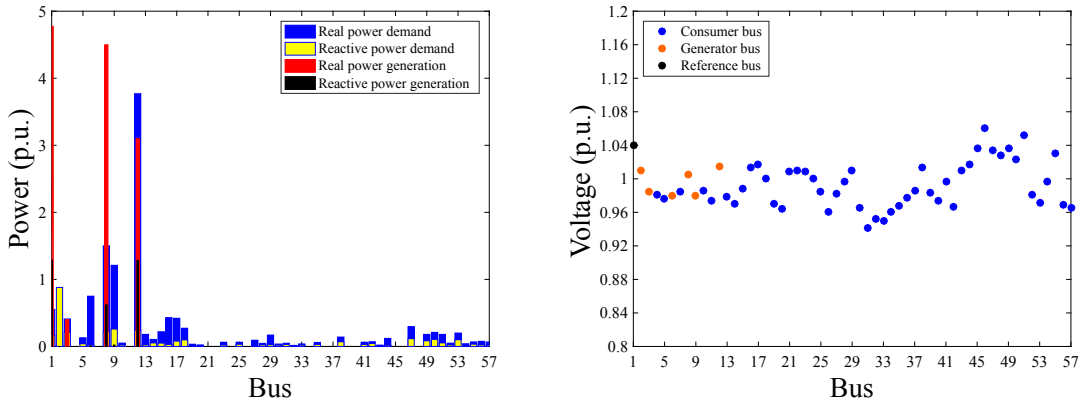

(a) Power flow data (b) Voltage profile without PV generation

Figure 5.10: IEEE 57-bus power system

In the case of uniform distribution of PV generators, net power generation of PV is scanned from 10% to 70% of net consumer real power demand. The associated analysis results of least-square method and LASSO method are shown in Figure 5.11. Average MSE in Figure 5.11a of the two methods result in nearly same value as zero, which means both methods suppress voltage deviation towards the reference voltage. Average VSM in both methods decrease with respect to the increase of net power generation from PV. Although control performances of both methods are nearly the

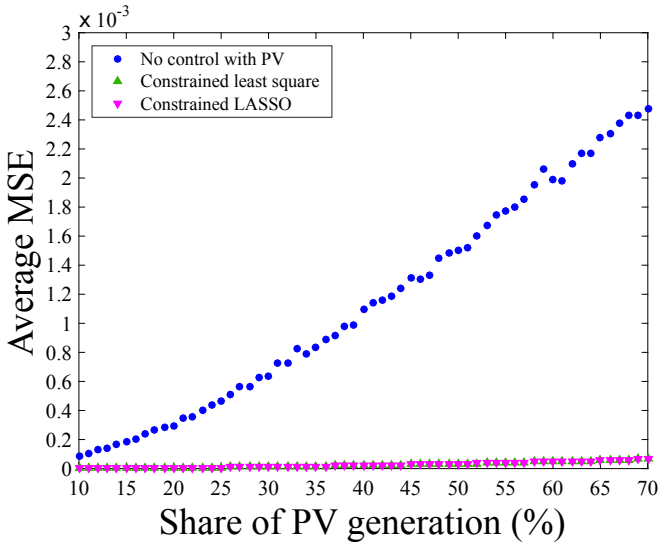

(a) Average MSE of voltage

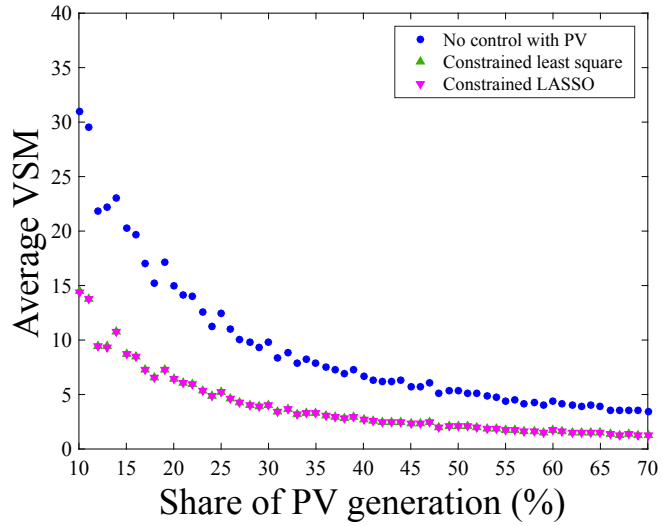

(b) Average VSM

Figure 5.11: Uniform distribution of PV generators in 57-bus power system

same, control cost, average RP shown in Figure 5.11c, in LASSO method is constantly lower than that in the least-square method.

In the case of on-demand distribution of PV generators, power generation from each PV is scanned from 10% to 70% of local consumer real power demand. Precision of voltage regulation shown in Figure 5.12a diverges with respect to the increase of

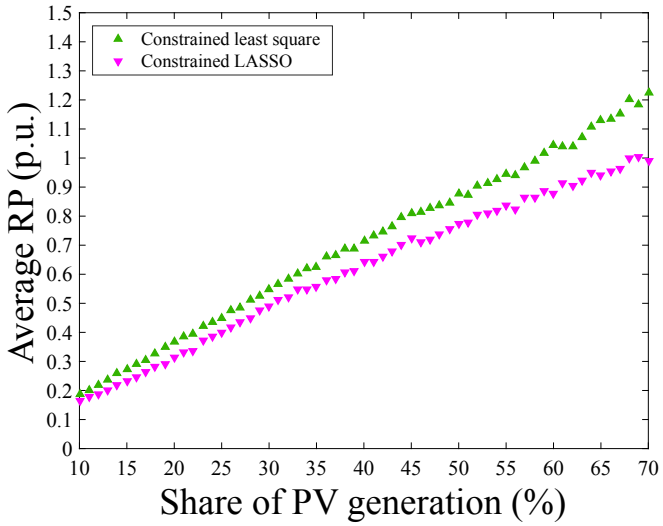

(c) Average RP

Figure 5.11: (Continued)

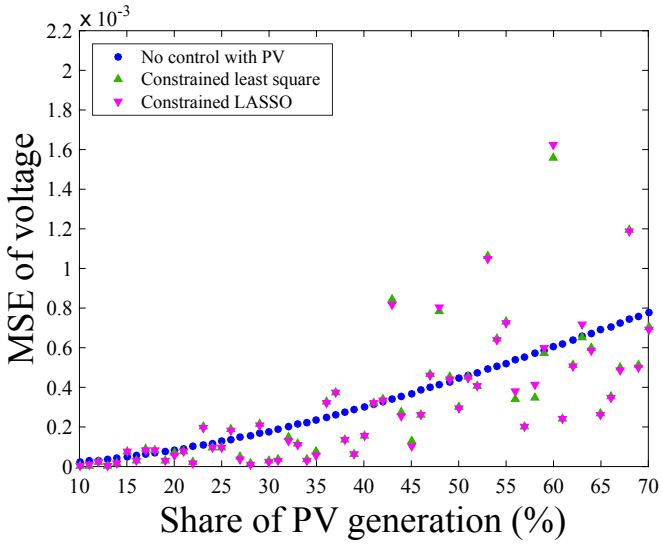

(a) MSE of voltage

Figure 5.12: On-demand distribution of PV generators in 57-bus power system

PV generation. Same tendencies occurs with VSM. Control cost of RP in Figure 5.12c indicate that LASSO constantly solve the control problem with lower inverter reactive power injection. Although control performances worsen in the on-demand

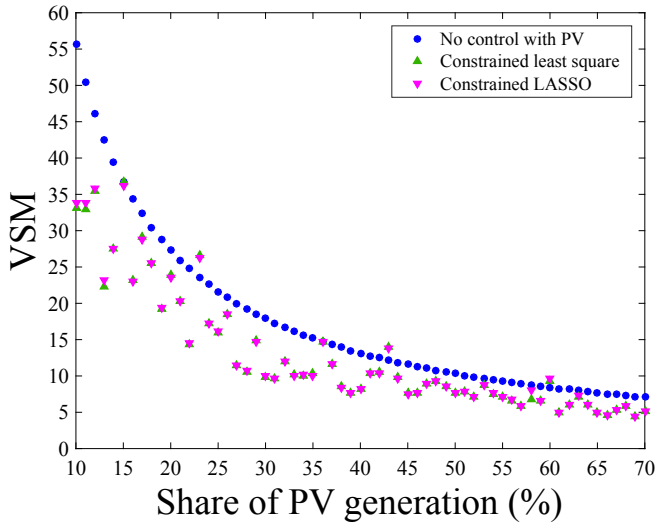

(b) VSM

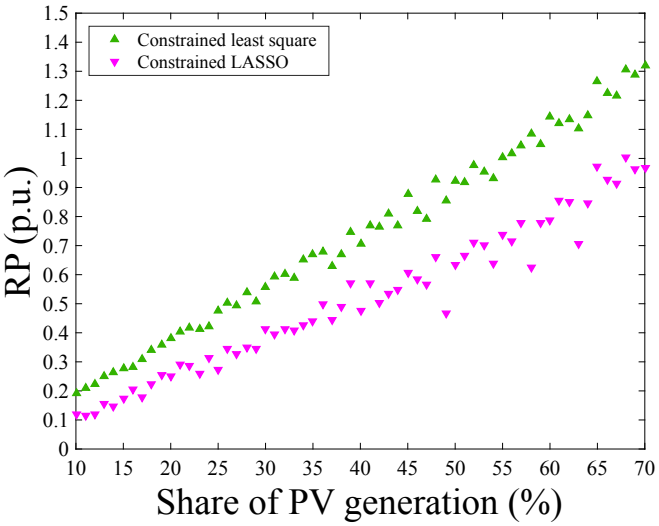

(c) RP

Figure 5.12: (Continued)

case, the least-square and LASSO method result in the same performances on voltage regulation, which hint that proper design of reference voltage or control model may improve their control performances. The power losses in the 57-bus power system are shown in Figure 5.13, where the power losses in the uniform distribution case are higher than the on-demand distribution case. The different tendency of power losses

in 39-bus and 57-bus power system indicates the configuration of power networks, power flow data and integration patterns of PV all impact on the power losses of PV-enabled power system.

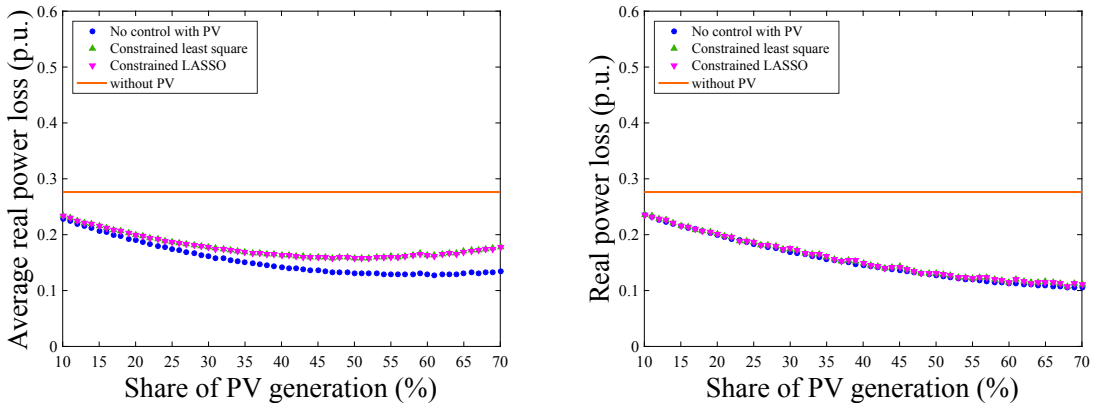

(a) Uniform distribution of PV generators (b) On-demand distribution of PV generators

Figure 5.13: Power losses in IEEE 57-bus power system

5.5 Summary

In this chapter, an efficient control scheme of inverter reactive power is proposed for power system with high and random PV generation. A constrained linear model is derived from power flow equations of meshed power system, which describes voltage magnitude change and PV inverter reactive power change subject to constraint of inverter capability. Control problem is formulated as to optimize the best fit of inverter reactive power that minimizing voltage variation. Constrained LASSO method is adopted on the control problem. The constrained LASSO method modifies the standard least-square method by adding a ℓ^1-norm penalty on the reactive power change, which contributes to shrink the estimated solution of reactive power injection towards zero. The application of constrained LASSO method aims to select the least essential PV inverters for voltage regulation, without sacrificing performance of voltage control. For comparison, control problem is also solved with standard least-square method. The associated results of constrained least-square and LASSO are evaluated with three indices: net absolute reactive power generation of PV inverters (RP), voltage stability margin (VSM) and mean square error of voltage magnitude (MSE). IEEE 39-bus and 57-bus power systems are taken as benchmark examples for evaluating the proposed control method. The analysis results show that the constrained LASSO approach succeeds in obtaining sparse solutions for distributed reactive power control,

which enables to select the minimum required number of inverters for voltage regulation without losing control performance. To further improve voltage regulation quality, the proper design of the reference voltage in the control schemes, comparison of other types of local control schemes for inverters are left for future research. Also, the ultimate goal of voltage regulation with inverter reactive power is considered to convert the centralized control scheme into decentralized control scheme, which enables the control performance of centralized control based on local consumer information.

Chapter 6

Conclusion

The massive promotion of PV generators brings benefits as well as technical challenges in the existing power system. One of the major concerns is voltage stability when large number of PV generators randomly connects with power system. Reactive power control of PV inverter has been considered a fast and efficient approach for rapid PV deployment. This work aims to investigate voltage stability of power system under large and random PV allocation and inverter control, as well as to propose effective reactive power control scheme to sustain voltage stability.

Statistical and worst-case analysis of voltage stability were conducted in radial distribution system. Two cases of PV allocation patterns were designed: random distribution of fixed number of PV generators; uniform distribution of large number of PV generators. Basic control schemes of inverter reactive power were applied on PV. Analyses results showed that allocation patterns of PV influences the changes of voltage profiles; Severe deviation of nodal voltages often occurs at the tail part of a circuit line. In addition, the upper stream of lateral circuit lines that near the system generator, turns out to be sensitive to the PV integration. As voltage profiles at these parts are usually higher than the tail part in the absence of PV, power generation from PV easily rises the voltage beyond its upper operating limit. Furthermore, inverter reactive power control regulates voltage deviation in certain extent. However, The voltage stability may be spoiled under certain PV allocation patterns.

The analyses results shown above motivated the author to conduct the inverter reactive power control from a centralized control approach, which cares for the allocations of both PV generators and reactive power injection of inverters. A constrained linear model between voltage magnitude change and reactive power change was derived from power flow equations of PV-enabled power system. The control problem was formulated as two types of optimization problem: One is standard constrained least-square method, which aims to find the best fit of reactive power

output with respect to an objective voltage change. The other is named as constrained LASSO method that adds a ℓ^1-norm penalty to its regression coefficients. The ℓ^1-norm penalty contributed to select the least essential inverters for voltage regulation, meanwhile, sustained its control efforts as that of the constrained least-square method. Meshed network power system was taken to conduct the analysis on control effects of constrained LASSO method. Constrained LASSO optimization technique succeeded in suppressing voltage deviation towards reference voltage, with essential PV inverters.

References

[1] J Duncan Glover, Mulukutla S Sarma, and Thomas Overbye. *Power System Analysis & Design, SI Version*. Cengage Learning, 2012.

[2] Ali Keyhani, Mohammad N Marwali, and Min Dai. *Integration of green and renewable energy in electric power systems*. John Wiley & Sons, 2009.

[3] Janaka B Ekanayake, Nick Jenkins, Kithsiri Liyanage, Jianzhong Wu, and Akihiko Yokoyama. *Smart grid: technology and applications*. John Wiley & Sons, 2012.

[4] Gilbert M Masters. *Renewable and efficient electric power systems*. John Wiley & Sons, 2013.

[5] REN21. Renewables 2017 global status report. Technical report, REN21 Secretariat, 2017.

[6] Brian Vad Mathiesen, Henrik Lund, David Connolly, Henrik Wenzel, Poul Alberg Østergaard, Bernd Möller, Steffen Nielsen, Iva Ridjan, Peter Karnøe, Karl Sperling, et al. Smart energy systems for coherent 100% renewable energy and transport solutions. *Applied Energy*, 145:139–154, 2015.

[7] REN21. Renewables global futures report: great debates towards 100% renewable energy. Technical report, REN21 Secretariat, 2017.

[8] Cedric Philibert, Paolo Frankl, Cecilia Tam, Yasmina Abdelilah, Heymi Bahar, Quentin Marchais, Simon Mueller, Uwe Remme, Micheal Waldron, and Hoel Wiesner. Technology roadmap solar photovoltaic energy. Technical report, International Energy Agency, 2014.

[9] RA Walling, Robert Saint, Roger C Dugan, Jim Burke, and Ljubomir A Kojovic. Summary of distributed resources impact on power delivery systems. *IEEE Transactions on power delivery*, 23(3):1636–1644, 2008.

[10] Eilyan Bitar, Pramod P Khargonekar, and Kameshwar Poolla. Systems and control opportunities in the integration of renewable energy into the smart grid. *IFAC Proceedings Volumes*, 44(1):4927–4932, 2011.

[11] Lori Bird, Michael Milligan, and Debra Lew. Integrating variable renewable energy: challenges and solutions. *National Renewable Energy Laboratory*, 2013.

[12] Simon Mueller, Paolo Frankl, and Keisuke Sadamori. Next generation wind and solar power from cost to value. Technical report, International Energy Agency, 2016.

[13] Philip P Barker and Robert W De Mello. Determining the impact of distributed generation on power systems. i. radial distribution systems. In *Power Engineering Society Summer Meeting, 2000. IEEE*, volume 3, pages 1645–1656. IEEE, 2000.

[14] M Begović, A Pregelj, A Rohatgi, and D Novosel. Impact of renewable distributed generation on power systems. In *In Proceeding of the 34th Hawaii International Conference on System Sciences, Maui, Hawaii*, pages 2001–2008, 3–6 January 2001.

[15] Reginald Comfort, A Mansoor, and A Sundaram. Power quality impact of distributed generation: effect on steady state voltage regulation. In *In Proceeding of the PQA 2001 North America Conference, Pittsburgh, PA, USA*, 2–7 June, 2001.

[16] Y Liu, Jovan Bebic, B Kroposki, J De Bedout, and W Ren. Distribution system voltage performance analysis for high-penetration pv. In *Energy 2030 Conference, 2008. ENERGY 2008. IEEE*, pages 1–8. IEEE, 2008.

[17] Ben Kroposki, Robert Margolis, G Kuswa, J Torres, W Bower, T Key, and D Ton. Renewable systems interconnection: Executive summary. Technical report, National Renewable Energy Laboratory (NREL), Golden, CO., 2008.

[18] Yaosuo Xue, Madhav Manjrekar, Chenxi Lin, Maria Tamayo, and John N Jiang. Voltage stability and sensitivity analysis of grid-connected photovoltaic systems. In *Power and Energy Society General Meeting, 2011 IEEE*, pages 1–7. IEEE, 2011.

[19] J Bank, B Mather, J Keller, and M Coddington. High penetration photovoltaic case study report. Technical report, National Renewable Energy Laboratory (NREL), Golden, CO., 2013.

[20] Prabha Kundur, John Paserba, Venkat Ajjarapu, Göran Andersson, Anjan Bose, Claudio Canizares, Nikos Hatziargyriou, David Hill, Alex Stankovic, Carson Taylor, et al. Definition and classification of power system stability ieee/cigre joint task force on stability terms and definitions. *IEEE transactions on Power Systems*, 19(3):1387–1401, 2004.

[21] Jan Machowski, Janusz Bialek, and Jim Bumby. *Power system dynamics: stability and control*. John Wiley & Sons, 2011.

[22] Fabio Saccomanno. *Electric Power Systems: Analysis and Control*. Wiley-IEEE Press, 1 edition, 2 2003.

[23] Angelo Baggini. *Handbook of power quality*. John Wiley & Sons, 2008.

[24] P Kessel and H Glavitsch. Estimating the voltage stability of a power system. *IEEE Transactions on Power Delivery*, 1(3):346–354, 1986.

[25] Sumit Paudyal, Claudio A Canizares, and Kankar Bhattacharya. Optimal operation of distribution feeders in smart grids. *IEEE Transactions on Industrial Electronics*, 58(10):4495–4503, 2011.

[26] Mesut E Baran and Ismail M El-Markabi. A multiagent-based dispatching scheme for distributed generators for voltage support on distribution feeders. *IEEE Transactions on power systems*, 22(1):52–59, 2007.

[27] Duong Quoc Hung, Nadarajah Mithulananthan, and RC Bansal. Analytical expressions for dg allocation in primary distribution networks. *IEEE Transactions on energy conversion*, 25(3):814–820, 2010.

[28] Fahad S Abu-Mouti and ME El-Hawary. Optimal distributed generation allocation and sizing in distribution systems via artificial bee colony algorithm. *IEEE transactions on power delivery*, 26(4):2090–2101, 2011.

[29] M Ettehadi, H Ghasemi, and S Vaez-Zadeh. Voltage stability-based dg placement in distribution networks. *ieee transactions on power delivery*, 28(1):171–178, 2013.

[30] Carmen LT Borges and Djalma M Falcão. Impact of distributed generation allocation and sizing on reliability, losses and voltage profile. In *Power Tech Conference Proceedings, 2003 IEEE Bologna*, volume 2, pages 5–pp. IEEE, 2003.

[31] Antonio Luque and Steven Hegedus. *Handbook of photovoltaic science and engineering*. John Wiley & Sons, 2011.

[32] John A Duffie and William A Beckman. *Solar engineering of thermal processes*. John Wiley & Sons, 2013.

[33] Sara Eftekharnejad, Vijay Vittal, Gerald Thomas Heydt, Brian Keel, and Jeffrey Loehr. Impact of increased penetration of photovoltaic generation on power systems. *IEEE Transactions on Power Systems*, 28(2):893–901, 2013.

[34] M Braun. Reactive power supplied by pv inverters–cost-benefit-analysis. In *22nd European Photovoltaic Solar Energy Conference and Exhibition*, pages 3–7, 2007.

[35] Masoud Farivar, Christopher R Clarke, Steven H Low, and K Mani Chandy. Inverter var control for distribution systems with renewables. In *Smart Grid Communications (SmartGridComm), 2011 IEEE International Conference on*, pages 457–462. IEEE, 2011.

[36] Hen-Geul Yeh, Dennice F Gayme, and Steven H Low. Adaptive var control for distribution circuits with photovoltaic generators. *IEEE Transactions on Power Systems*, 27(3):1656–1663, 2012.

[37] Pedram Jahangiri and Dionysios C Aliprantis. Distributed volt/var control by pv inverters. *IEEE Transactions on power systems*, 28(3):3429–3439, 2013.

[38] Ganbayar Puntsagdash. Stability analysis with decentralized control of photovoltaic systems. *Master's Thesis, Swiss Federal Institute of Technology (ETH)*, 2013.

[39] B Seal. Standard language protocols for photovoltaics and storage grid integration. *Electric Power Research Institute (EPRI), Tech. Rep*, 2010.

[40] Konstantin Turitsyn, Petr Sulc, Scott Backhaus, and Michael Chertkov. Options for control of reactive power by distributed photovoltaic generators. *Proceedings of the IEEE*, 99(6):1063–1073, 2011.

[41] Erhan Demirok, Pablo Casado Gonzalez, Kenn HB Frederiksen, Dezso Sera, Pedro Rodriguez, and Remus Teodorescu. Local reactive power control methods for overvoltage prevention of distributed solar inverters in low-voltage grids. *IEEE Journal of Photovoltaics*, 1(2):174–182, 2011.

[42] Md Jan E Alam, Kashem M Muttaqi, and Danny Sutanto. A multi-mode control strategy for var support by solar pv inverters in distribution networks. *IEEE transactions on power systems*, 30(3):1316–1326, 2015.

[43] Masoud Farivar, Russell Neal, Christopher Clarke, and Steven Low. Optimal inverter var control in distribution systems with high pv penetration. In *Power and Energy Society General Meeting, 2012 IEEE*, pages 1–7. IEEE, 2012.

[44] Sergios Theodoridis and Konstantinos Koutroumbas. *Pattern Recognition, Fourth Edition*. Academic Press, 4 edition, 11 2008.

[45] Yu Li and Masato Ishikawa. Sensitivity analysis of radially distributed power system under random penetration of photovoltaic generation. In *10th AsianControl Conference (ASCC)*, pages 1–6. IEEE, 2015.

[46] Yu Li and Masato Ishikawa. Statistical analysis of power system sensitivity under random penetration of photovoltaic generation. *Asian Journal of Control*, 2017.

[47] Thomas S Basso and Richard DeBlasio. IEEE 1547 series of standards: interconnection issues. *IEEE Transactions on Power Electronics*, 19(5):1159–1162, 2004.

[48] Thomas Basso and Richard DeBlasio. Ieee smart grid series of standards ieee 2030 (interoperability) and ieee 1547 (interconnection) status. *Grid-Interop*, pages 5–8, 2011.

[49] Baofu Gao, GK Morison, and Prabhashankar Kundur. Voltage stability evaluation using modal analysis. *IEEE transactions on power systems*, 7(4):1529–1542, 1992.

[50] Brian R Gaines and Hua Zhou. Algorithms for fitting the constrained lasso. *arXiv preprint arXiv:1611.01511*, 2016.

[51] Gareth M James, Courtney Paulson, and Paat Rusmevichientong. The constrained lasso. Technical report, Citeseer, 2012.

[52] Robert Tibshirani. Regression shrinkage and selection via the lasso. *Journal of the Royal Statistical Society. Series B (Methodological)*, pages 267–288, 1996.

[53] Bradley Efron, Trevor Hastie, Iain Johnstone, Robert Tibshirani, et al. Least angle regression. *The Annals of statistics*, 32(2):407–499, 2004.

[54] Yu Li and Masato Ishikawa. An efficient reactive power control method for power network systems with solar photovoltaic generators using sparse optimization. *Energies*, 10(5):696, 2017.

[55] Samir Kouro, Jose I Leon, Dimitri Vinnikov, and Leopoldo G Franquelo. Grid-connected photovoltaic systems: An overview of recent research and emerging pv converter technology. *IEEE Industrial Electronics Magazine*, 9(1):47–61, 2015.

[56] Roger Messenger and Amir Abtahi. *Photovoltaic systems engineering*. CRC press, 2017.

[57] Widalys De Soto, SA Klein, and WA Beckman. Improvement and validation of a model for photovoltaic array performance. *Solar energy*, 80(1):78–88, 2006.

[58] Jenny Nelson. *The physics of solar cells*. World Scientific Publishing Co Inc, 2003.

[59] Pallavee Bhatnagar and RK Nema. Maximum power point tracking control techniques: State-of-the-art in photovoltaic applications. *Renewable and Sustainable Energy Reviews*, 23:224–241, 2013.

[60] Soumya Kundu, Scott Backhaus, and Ian A Hiskens. Distributed control of reactive power from photovoltaic inverters. In *Circuits and Systems (ISCAS), 2013 IEEE International Symposium on*, pages 249–252. IEEE, 2013.

[61] Abdelhay A Sallam and Om P Malik. *Electric distribution systems*, volume 68. John Wiley & Sons, 2011.

[62] ME Baran and Felix F Wu. Optimal sizing of capacitors placed on a radial distribution system. *IEEE Transactions on power Delivery*, 4(1):735–743, 1989.

[63] Mesut E Baran and Felix F Wu. Optimal capacitor placement on radial distribution systems. *IEEE Transactions on power Delivery*, 4(1):725–734, 1989.

[64] Mesut E Baran and Felix F Wu. Network reconfiguration in distribution systems for loss reduction and load balancing. *IEEE Transactions on Power delivery*, 4(2):1401–1407, 1989.

[65] Prabha Kundur, Neal J Balu, and Mark G Lauby. *Power system stability and control*, volume 7. McGraw-hill New York, 1994.

[66] Ray Daniel Zimmerman, Carlos Edmundo Murillo-Sánchez, and Robert John Thomas. Matpower: Steady-state operations, planning, and analysis tools for power systems research and education. *IEEE Transactions on power systems*, 26(1):12–19, 2011.

[67] B Venkatesh, S Chandramohan, N Kayalvizhi, and RP Kumudini Devi. Optimal reconfiguration of radial distribuion system using artificial intelligence methods. In *Science and Technology for Humanity (TIC-STH), 2009 IEEE Toronto International Conference*, pages 660–665. IEEE, 2009.

[68] Aleksandar Pregelj, Miroslav Begovic, and Ajeet Rohatgi. Quantitative techniques for analysis of large data sets in renewable distributed generation. *IEEE Transactions on Power Systems*, 19(3):1277–1285, 2004.

[69] Jiao-Jiao Deng and Hsiao-Dong Chiang. Convergence region of newton iterative power flow method: numerical studies. *Journal of Applied Mathematics*, 2013, 2013.

[70] Jerome Friedman, Trevor Hastie, and Robert Tibshirani. *The elements of statistical learning*, volume 1. Springer series in statistics Springer, Berlin, 2001.

[71] Anantha Pai. *Energy function analysis for power system stability*. Springer Science & Business Media, 2012.

[72] Rich Christie. IEEE 57-bus power system, 1993.

[73] Venkataramana Ajjarapu and Colin Christy. The continuation power flow: a tool for steady state voltage stability analysis. *IEEE transactions on Power Systems*, 7(1):416–423, 1992.

[74] Hsiao-Dong Chiang, Alexander J Flueck, Kirit S Shah, and Neal Balu. CPFLOW: A practical tool for tracing power system steady-state stationary behavior due to load and generation variations. *IEEE Transactions on Power Systems*, 10(2):623–634, 1995.

List of publications

Journal papers

1. Yu Li and Masato Ishikawa. Statistical Analysis of Power System Sensitivity Under Random Penetration of Photovoltaic Generation. *Asian Journal of Control*, 19(5), pages 1-11, 2017.
2. Yu Li and Masato Ishikawa. An Efficient Reactive Power Control Method for Power Network Systems with Solar Photovoltaic Generators Using Sparse Optimization. *Energies*, 10(5): 696, 2017.

International conference with full-review

1. Daisuke Nakanishi, Yuichiro Sueoka, Yu Li, Yasuhiro Sugimoto, Masato Ishikawa, Koichi Osuka, Yoshiyuki Sankai. Emergence and motion analysis of 3D quasi-passive dynamic walking by excitation of lateral rocking. In *Proceedings of 2012 IEEE/RSJ International Conference on Intelligent Robots and Systems (IROS)*, pages 2769-2774, Vilamoura, Portugal, 7-12 October 2012.
2. Kentaro Oki, Masato Ishikawa, Yu Li, Naoto Yasutani, and Koichi Osuka. Tripedal walking robot with fixed coxa driven by radially stretchable legs. In *Proceedings of 2015 IEEE/RSJ International Conference on Intelligent Robots and Systems (IROS)*, pages 5162-5167, Hamburg, Germany, 28 September-2 October 2015.
3. Yu Li and Masato Ishikawa. Sensitivity analysis of radially distributed power system under random penetration of photovoltaic generation. In *Proceedings of 10th Asian Control Conference (ASCC)*, pages 1-6, Kota Kinabalu, Malaysia, 31 May-3 June 2015.

Domestic conference

1. Yu Li, Yasuhiro Sugimoto, Yuichiro Sueoka, Koichi Osuka and Yoshiyuki Sankai. On gait of a 3-link under-actuated bipedal walking robot. In *Proceedings of the Annual Conference of the Institute of Systems, Control and Information Engineers*, pages 295-296, Kyoto, Japan, 21-23 May, 2012.
2. Yu Li, Yasuhiro Sugimoto and Koichi Osuka. On gait efficiency of 3-link under-actuated bipedal walking robot. In *Proceedings of 2013 JSME The Robotics and Mechatronics Conference*, Tsukuba, Japan, 22-25 May 2013.
3. Tetsuya Yoshikawa, Yuichiro Sueoka, Yu Li and Masato Ishikawa. On synchronization of noise-driven nonlinear oscillator network. In *Proceedings of the Annual Conference of the Institute of System, Control and Information Engineers*, pages 341-343, Kyoto, Japan, 21-23 May 2014.